

12

AFGL-TR-83-0080
ENVIRONMENTAL RESEARCH PAPERS, NO. 831



**Winds: Chapter 6, 1983 Revision,
Handbook of Geophysics and Space Environments**

ALLEN E. COLE
DONALD D. GRANTHAM
IRVING I. GRINGORTEN
ARTHUR J. KANTOR
PAUL TATTELMAN

21 March 1983

Approved for public release; distribution unlimited.

DTIC
ELECTE
SEP 01 1983

METEOROLOGY DIVISION PROJECT 6670
AIR FORCE GEOPHYSICS LABORATORY
HANSCOM AFB, MASSACHUSETTS 01731

AIR FORCE SYSTEMS COMMAND, USAF



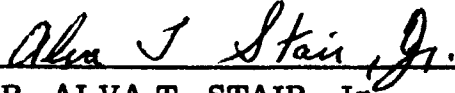
ADA 132018

DTIC FILE COPY

83 08 31 007

This report has been reviewed by the ESD Public Affairs Office (PA) and is releasable to the National Technical Information Service (NTIS).

This technical report has been reviewed and is approved for publication.



DR. ALVA T. STAIR, Jr
Chief Scientist

Qualified requestors may obtain additional copies from the Defense Technical Information Center. All others should apply to the National Technical Information Service.

Unclassified

SECURITY CLASSIFICATION OF THIS PAGE (When Data Entered)

REPORT DOCUMENTATION PAGE		READ INSTRUCTIONS BEFORE COMPLETING FORM
1 REPORT NUMBER AFGL-TR-83-0080	2. GOVT ACCESSION NO.	3. RECIPIENT'S CATALOG NUMBER
4 TITLE (and Subtitle) WINDS: CHAPTER 6, 1983 REVISION, HANDBOOK OF GEOPHYSICS AND SPACE ENVIRONMENTS		5. TYPE OF REPORT & PERIOD COVERED Scientific. Interim.
		6 PERFORMING ORG. REPORT NUMBER ERP, No. 831
7 AUTHOR(s) Allen E. Cole Arthur J. Kantor Donald D. Grantham Paul Tattelman Irving I. Gringorten		8 CONTRACT OR GRANT NUMBER(s)
9 PERFORMING ORGANIZATION NAME AND ADDRESS Air Force Geophysics Laboratory (LY) Hanscom AFB Massachusetts 01731		10. PROGRAM ELEMENT, PROJECT, TASK AREA & WORK UNIT NUMBERS 62101F 66700910
11 CONTROLLING OFFICE NAME AND ADDRESS Air Force Geophysics Laboratory (LY) Hanscom AFB Massachusetts 01731		12. REPORT DATE 21 March 1983
		13 NUMBER OF PAGES 66
14 MONITORING AGENCY NAME & ADDRESS (if different from Controlling Office)		15 SECURITY CLASS (of this report) Unclassified
		15a. DECLASSIFICATION/DOWNGRADING SCHEDULE
16 DISTRIBUTION STATEMENT (of this Report) Approved for public release; distribution unlimited.		
17 DISTRIBUTION STATEMENT (of the abstract entered in Block 20, if different from Report)		
18 SUPPLEMENTARY NOTES		
19 KEY WORDS (Continue on reverse side if necessary, and identify by block number) Wind Wind structure Wind as a function of height Wind profiles		
20 ABSTRACT (Continue on reverse side if necessary and identify by block number) This report is a revision of Chapter 4 of the 1965 Edition, Handbook of Geophysics and Space Environments. The need for geophysical and astrophysical information is critical to the design of aircraft, missiles, and satellites. The Handbook of Geophysics and Space Environments is an attempt by the U. S. Air Force to organize some of these data into one source. Winds, surface to 90 km, are discussed in this Chapter. Information on winds as a function of height, large scale wind structure, wind profiles, and design data on winds are included.		

DD FORM 1 JAN 73 1473 EDITION OF 1 NOV 65 IS OBSOLETE

Unclassified

SECURITY CLASSIFICATION OF THIS PAGE (When Data Entered)

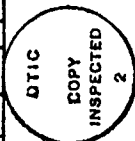
Preface

This report is a revision of Chapter 4 of the Handbook of Geophysics and Space Environments. * (Numbers of Sections are not the same as those in the original Handbook, therefore the cross-referencing systems to other chapters are not valid.

We thank Mrs. Helen Connell for typing this report.

*Published by the Air Force Cambridge Research Laboratories and by the McGraw-Hill Book Co. in 1965.

Accession For	
NTIS GRA&I	<input checked="" type="checkbox"/>
DTIC TAB	<input type="checkbox"/>
Unannounced	<input type="checkbox"/>
Justification	
By _____	
Distribution/	
Availability Codes	
Dist	Avail and/or Special
A	



Contents

6.1	INTRODUCTION	9
6.2	WINDS AS A FUNCTION OF HEIGHT, by Irving I. Gringorten and Donald D. Grantham	10
6.2.1	Variation of Wind Speed With Height (Lowest 100 meters)	11
6.2.2	Wind Duration Shift (Below 3,000 meters)	16
6.2.3	Diurnal Variation and Low-Level Jet Streams (Below 2,000 meters)	19
6.3	LARGE SCALE WIND STRUCTURE, by Arthur J. Kantor and Allen E. Cole	22
6.3.1	Seasonal and Day-to-Day Variations	22
6.3.2	Time and Space Variations	28
6.3.2.1	Time Variability up to 30 km	29
6.3.2.2	Spatial Variability up to 30 km	33
6.3.2.3	Time and Space Variations - 30 to 60 km	33
6.4	WIND PROFILES, by Arthur J. Kantor and Allen E. Cole	36
6.4.1	Wind Shear	36
6.4.2	Interlevel Correlations	42
6.5	DESIGN DATA ON WINDS, by Irving I. Gringorten and Paul Tattelman	46
6.5.1	Hourly Surface Wind Speeds	46
6.5.2	Surface Wind Direction	51
6.5.3	Surface Wind Gusts	52
6.5.4	Extreme Surface Wind Speeds	57
6.5.5	Structure of Jet Streams	62
	REFERENCES	65

Illustrations

6. 1.	A Nomogram to Obtain Windspeeds of Duration 1 to 1000 Sec at a Height of 1 to 32 Meters	15
6. 2.	Diurnal Curves (slightly smoothed) of Annual Mean Wind Speed at Oak Ridge, Tennessee, Average for 1948 to 1952	20
6. 3.	Meridional Cross Section of Zonal Wind Speed (m/sec)	23
6. 4.	Annual Variation of Meridional and Zonal Wind at White Sands, Wallops Island and Fort Churchill	24
6. 5a.	Seasonal Effects on the Zonal Wind Profiles at Ascension Island, Wallops Island and Churchill	25
6. 5b.	Seasonal Effects on the Meridional Wind Profiles at Ascension Island, Wallops Island and Churchill	26
6. 6a.	Day-to-Day Variability Around Mean Monthly Zonal Winds for the Midseason Months at Ascension Island, Wallops Island and Churchill	27
6. 6b.	Day-to-Day Variability Around Mean Monthly Meridional Winds for the Midseason Months at Ascension Island, Wallops Island and Churchill	27
6. 7.	Isopleths of Time and Space Variabilities of Changes in the Mean Vector Wind With Altitude	28
6. 8.	Distribution in Latitude and Altitude of the Vector Wind Wind Variability (St) for a 24-hr Time Lag Between Observations Along the Meridian 75°W in Summer and Winter	31
6. 9a.	Diurnal Wind Variations at Wallops Island in May (N-S)	34
6. 9b.	Diurnal Wind Variations at Wallops Island in May (E-W)	35
6. 10.	RMS Differences Between North-South Winds Observed 1 to 72 hr Apart in the Tropics	36
6. 11.	Selected Vertical Wind Shear Spectrums (4-, 10-, to 14-, 20- to 35-, and 60- to 80-km Altitude) for Use With 5 Percent and 1 Percent Probability Level Wind Profile Envelope, Cape Kennedy, Florida	37
6. 12.	One Percent Probability-of-Occurrence Vertical Wind Shear Spectrum as Function of Altitude and Scale-of-Distance for Association With the 5 Percent and 1 Percent Wind Speed Profile Envelope for Cape Kennedy, Florida	38
6. 13.	Curves of the 30-sec and 1-min Gust Factor to 5-min Wind Speed for the Airfield Data Fitted to $GF = 1 + Ae^{-Bv}$	53
6. 14.	Relationship Between the 2-sec Gust Factor and the 5-min Wind Speed at Indicated Percentiles for the Airfield Data	53
6. 15.	Expected (50-percentile) Gust Factors Versus Gust Duration and 5-min Steady Speed	54
6. 16.	Ninety Percentile Wind Speed Range Versus Time Interval and 5-min Speed	55
6. 17.	Idealized Model of the Jet Stream, Average Structure in a Cross Section Perpendicular to the Flow	56

Illustrations

6.18. Example of Wind and Temperature Fields Near the Jet Stream	57
6.19. Turbulence in Various Sectors of a Typical Jet Stream Cross Section	57

Tables

6.1. Ratio of Wind Speed at Height H to Speed at 91 m Over Open Prairie Obtained During the Great Plains Turbulence Field Program	11
6.2. Typical Values of the Roughness Parameter, H_0	12
6.3. Ratios of Wind at Height H to Wind at Height H_1 for Two Reference Levels and Three Roughness Parameters H_0 , Calculated by Eq. (6.1)	13
6.4. Mean Values, for Heights Ranging from 10 to 100 m, of Exponent p in Eq. (6.2)	14
6.5. Mean Values of Exponent (p) for the Lowest 9 m in Eq. (6.2), Determined From Wind Profile Measurements	14
6.6. Typical Frictional Veering of Wind Over Plain Land With Moderately Strong Gradient Winds (18 m/sec) and No Temperature Advection; 51.3°N, 12.5°E, 20 October 1931	17
6.7. Average Angle Formed by the Wind and the Gradient Wind, and Average Veering for Weather Stations in Germany, Grouped According to Topography	18
6.8. Average Veering (deg/100 m) for Various Ranges of Height; Means (1918 to 1920) for Three Stations in U. S. A. in the Latitude Zone 31° to 36° (average 33°N), and Three in Latitude Zone 40° to 45° (average 43°N)	18
6.9. Average Wind Profiles (speed and direction at various heights) Showing Development of Nocturnal Low-Level Jet Stream	21
6.10. Mean and Standard Deviation of Absolute Value of Vector Velocity Differences at Various Time Intervals, Δt , in the Lower 1829 m (600 ft) Over Smooth Open Terrain	30
6.11. Envelopes of 99 Percentile Wind Speed Change (m/sec), 1- to 80-km Altitude Region, Eastern Test Range	39
6.12. Envelopes of 99 Percentile Wind Speed Change (m/sec), 1- to 80-km Altitude Region, Vandenberg, AFB	39
6.13. Envelopes of 99 Percentile Wind Speed Change (m/sec), 1- to 80-km Altitude Region, Wallops Island	40
6.14. Envelopes of 99 Percentile Wind Speed Change (m/sec), 1- to 80-km Altitude Region, White Sands Missile Range	40

Tables

6. 15. Envelopes of 99 Percentile Wind Speed Change (m/sec), 1- to 80-km Altitude Region, Edward AFB	41
6. 16. Envelopes of 99 Percentile Wind Speed Change (m/sec), 1- to 80-km Altitude Region, for All Five Locations	41
6. 17a. Zonal Winds From the Surface to 60 km at Churchill	43
6. 17b. Zonal Winds From the Surface to 60 km at Wallops Island	44
6. 17c. Zonal Winds From the Surface to 60 km at Ascension Island	45
6. 18. Extreme Annual Wind Speed (fastest m/sec) at 15.2 m (50 ft) Above Ground at the Given Stations; A Denotes Airport Station	60

Winds: Chapter 6, 1983 Revision, Handbook of Geophysics and Space Environments

6.1 INTRODUCTION

The atmosphere's motions defy rigorous classification or modeling. The application of a particular feature of wind structure to a given engineering problem should be dictated by its physical dimensions. Extrapolation of data beyond its indicated limitations is risky. Local conditions may not always be well represented by the data in this chapter, and may produce extreme wind variations in excess of those presented, even when the local wind structure is free from perturbations such as fronts, thunderstorms, squalls, and so on. The practicing engineer should avail himself of applicable local meteorological records whenever possible. Information other than that given below is available through the various national weather services and the World Meteorological Organization (NOCD).¹ Special studies prepared by ETAC or AFGL might provide the best answers for specific design problems.

The measure of wind, in speed and direction, presents an immediate problem in the time interval for the observation. A conventional observation of wind speed is the wind travel in 1 min, 5 min, or 1 hr, that is the 1-min average, 5-min average, or 1-hr average. The current standard averaging time period in the United States is 1 min. In England and Canada a 10-min period is customary when wind

(Received for publication 16 March 1983)

1. Naval Oceanography Command, Detachment (1980) Guide to Standard Weather Summaries and Climatic Services, NAVAIR 50-1C-534, Asheville, N. C.

speed recorders are available, otherwise the averaging period is something over 15 sec. However, in published climatic data, hourly (60-min) averaged winds are often given.

As might be expected, the variance of the 1-min wind is greater than the variance of the 5-min wind, which is greater than that of the 1-hr wind, but not seriously so. On the other hand, wind speeds of shorter duration than 1 min are subject to significantly greater variability. When the wind speeds peak, between lulls, in 20 sec or less, they are conventionally termed gusts.

6.2 WINDS AS A FUNCTION OF HEIGHT

A major problem with pooling the various surface wind observations is in the determination of the best method or model for adjusting wind speeds to a common height above the surface. But once established the mode formula can be used to describe wind speed and gusts along a vertical profile in the lowest 50 or 100 m of the atmosphere.

Wind flows in response to pressure gradients in the atmosphere. Such pressure gradients change slowly with altitude, negligibly within the first 100 m. Yet the changes in wind speed with height are pronounced. Air motion near the surface does not obey the simple pressure gradient law. Anemometers near the ground may be hardly turning, whereas those on tall buildings or towers may show moderately strong, gusty winds. Kites may be difficult to launch, but once several hundred feet high, they may fly without difficulty.

Friction caused by terrain is one of the main factors affecting the horizontal wind speed up to an altitude known as the gradient level. At this height, 300 or 600 m, the pressure gradient is said to be dynamically balanced against two other influences: the earth's rotation and the curvature of the wind path. A theoretical wind speed that closely approximates the observed wind at gradient height can be computed from the isobaric spacing and curvature on surface weather maps.

The height of the gradient level and the velocity profile up to that level vary greatly, mainly with the type of surface and the stability of the air. Stability is chiefly a function of the temperature structure in the boundary layer. One extreme of temperature structure is represented by a superadiabatic lapse rate in which temperature decreases rapidly with altitude so that air displaced upward will continue upward because it is warmer than its surroundings. The opposite extreme is a negative lapse rate or inversion, in which temperature increases with height, so that air displaced upward is cooler than its surroundings and tends to sink back to its original level. A neutral condition (adiabatic) exists when the temperature lapse rate is such that a parcel of air, displaced vertically, will experience no

buoyant acceleration. In general, a neutral lapse rate is established by the turbulent mixing caused by strong winds at the surface.

A formerly popular model for the shift of wind speed and direction with altitude in the boundary layer, originally developed for ocean depth, is termed the Ekman Spiral. Since its introduction, micrometeorologists have studied the energy transfer and diffusion phenomena in the boundary layer, and have found improved empirical relationships to fit wind speed data gathered at various heights above ground. Table 6.1 shows the ratio of wind speed at various heights to that at 91 m over open prairies. Values are based on actual wind measurements taken during the Great Plains Turbulence Field Program conducted at O'Neill, Nebraska (Lettau and Davidson²). The ratios are shown for typical daytime lapse rates ($dT/dz < 0$), night-time ($dT/dz > 0$) and for isothermal conditions ($dT/dz = 0$).

Table 6.1. Ratio of Wind Speed at Height H to Speed at 91 m Over Open Prairie Obtained During the Great Plains Turbulence Field Program

H (m)	V_H/V_{91}		
	Lapse Rate ($dT/dz < 0$)	Inversion ($dT/dz > 0$)	Isothermal ($dT/dz = 0$)
91	1.000	1.000	1.000
30	0.965	0.689	0.872
21	0.944	0.608	0.829
15	0.915	0.538	0.792
9	0.866	0.452	0.733
6	0.825	0.403	0.686
3	0.749	0.339	0.604
1.5	0.662	0.275	0.518
0.6	0.556	0.231	0.424
0.3	0.470	0.200	0.336
0.15	0.383	0.166	0.300

6.2.1 Variation of Wind Speed With Height (Lowest 100 meters)

Two alternative classes of models have been used to estimate the increase of wind speed with height: logarithmic and power models.

2. Lettau, H. H., and Davidson, B. (Eds.) (1957) Exploring the Atmosphere's First Mile, Pergamon Press.

In one logarithmic model

$$V/V_1 = \ln(1+H/H_0)/\ln(1+H_1/H_0) \quad (6.1)$$

where V is the mean wind speed at height H , and V_1 is the mean wind speed at the reference level (H_1) (anemometer level) and H_0 is the roughness parameter: a length determined by the characteristic ground surface. The boundary condition at $H = 0$ is $V = 0$. This model has the advantage that the effect of terrain is included explicitly. Typical values for H_0 are given in Table 6.2. Table 6.3 lists (V/V_1) for a variety of roughness parameters (H_0), for two reference levels and for various heights (H).

Table 6.2 Typical Values of the Roughness Parameter, H_0

Type of Surface	H_0 (cm)
Smooth (mud flats, ice)	0.0009
Lawn, grass up to 1 cm	0.09
Downland, thin grass up to 10 cm	0.61
Thick grass, up to 10 cm	2.25
Thin grass, up to 240 cm	4.9
Thick grass, up to 240 cm	9.1

In the simplest power model the mean wind speed, V , at height H is approximated by

$$V/V_1 = (H/H_1)^p \quad (6.2)$$

where the exponent p depends on the height, terrain, thermal stratification and speed of the overall airflow. The parameter p is larger for rough ground, for altitudes below H_1 and for relatively small V_1 . It varies within limits approximately 0.05 to 0.08, and averages between 0.1 and 0.3. Table 6.4 lists mean values of p , determined for several locations and two types of terrain. Table 6.5 lists mean values of p that were determined for typical daytime ($dT/dz < 0$) and nighttime ($dT/dz > 0$) conditions in the lowest 9 m over open prairie country (Great Plains Turbulence Field Program). The exponent p is larger when there is a stabilizing

inversion and smaller when there is a positive lapse rate. According to Sherlock³ a typical value for p is $1/7$ (or 0.143). Early workers had recognized that his p -value was applicable to typical steady or mean winds but not applicable to gustiness. Sherlock³ noted that gusts were better described with a value of $p = 0.0625$. Shellard⁴ in reducing high wind speeds and gusts to a common height of 10 m, used Eq. (6.2) with $p = 0.17$ for mean speeds and 0.085 for gusts.

Table 6.3. Ratios of Wind at Height H to Wind at Height H_1 for Two Reference Levels and Three Roughness Parameters H_0 . Calculated by Eq. (6.1)

H (m)	$H_0 = 30$ cm	$H_0 = 3$ cm	$H_0 = 0.3$ cm
V/V_1 for $H_1 = 6$ meters			
100	1.91	1.53	1.37
10	1.16	1.10	1.07
1	0.48	0.67	0.76
0.5	0.32	0.54	0.67
V/V_1 for $H_1 = 3$ meters			
100	2.42	1.76	1.51
10	1.47	1.26	1.17
1	0.61	0.77	0.84
0.5	0.41	0.62	0.74

A special study was made with data from the Windy Acres Project (Izumi⁵) consisting of 39 hr of 1-sec wind speeds, taken in the summer of 1968, at eight heights on a 32-m tower in southeast Kansas. The terrain was very flat and partly covered with wheat stubble 16 to 22 cm tall. The 1-sec wind (regrettably) was never more than 15.3 m/sec, Figure 6.1 (right side) presents resulting isopleths of p as a function of windspeed, from 1-sec winds including gusts to 1-hr integrated

3. Sherlock, R. H. (1952) Variation of wind velocity and gusts with height, Paper No. 2553, Proc. Am. Soc. Civil Eng. 1:463-508.
4. Shellard, H. C. (1965) The estimation of design wind speeds, Wind Effects on Buildings and Structures, National Physics Laboratory Symposium 16:30-51.
5. Izumi, Y. (1971) Kansas 1968 Field Program, ERP No. 379, AFCRL-72-0041, AD 739165.

Table 6.4. Mean Values for Heights Ranging From 10 to 100 meters. of Exponent p in Eq. (6.2)

Location and Terrain	p
FAIRLY LEVEL OPEN COUNTRY	
Ann Arbor, Michigan	0.14
Sale, Victoria, Australia	0.16
Cardington, Bedfordshire, England	0.17
Leafield, Oxfordshire, England	0.17
FAIRLY LEVEL WOODED COUNTRY	
Quickborn, Germany	0.23
Upton, Long Island, New York	0.26
Akron, Ohio	0.22

Table 6.5. Mean Values of Exponent (p) for the Lowest 9 meters in Eq. (6.2), Determined From Wind Profile Measurements

H (m)	p		
	Lapse Rate (dT/dz < 0)	Inversion (dT/dz > 0)	Isothermal (dT/dz = 0)
9	0.11	0.38	0.14
4.6	0.13	0.31	0.16
0.9	0.18	0.23	0.21

wind speeds. The exponents (1) were found for wind speeds of the same probability, from level to level, as opposed to the mean wind speed. Nevertheless previous results were supported. There is a systematic decrease of p, from 0.7 down to 0.12, with increasing wind speed for either 1-sec, 1-min, 5-min or 1-hr winds, when the lower 90 percent of the wind speeds are considered. For winds equal to or greater than the 90-percentiles the exponent (p) is almost uniform at 0.12 except for gusts or short-duration winds of 1-min or less. The Windy Acres winds became turbulent above the 95 percent speeds. In gusts the value of p varies from 0.11 down to 0.08, suggesting a tendency toward a common speed throughout the turbulent layer.

Briefly, Eq. (6.2) may be used to standardize the height of the wind data of individual stations to one level even though they have differing anemometer levels In the publication "Climatic Extremes for Military Equipment" (MIL-STD-210B)

the value of the exponent (p) was adopted at 0.125 when the wind is strong but steady, and at 0.08 when the wind is strong and gusty.

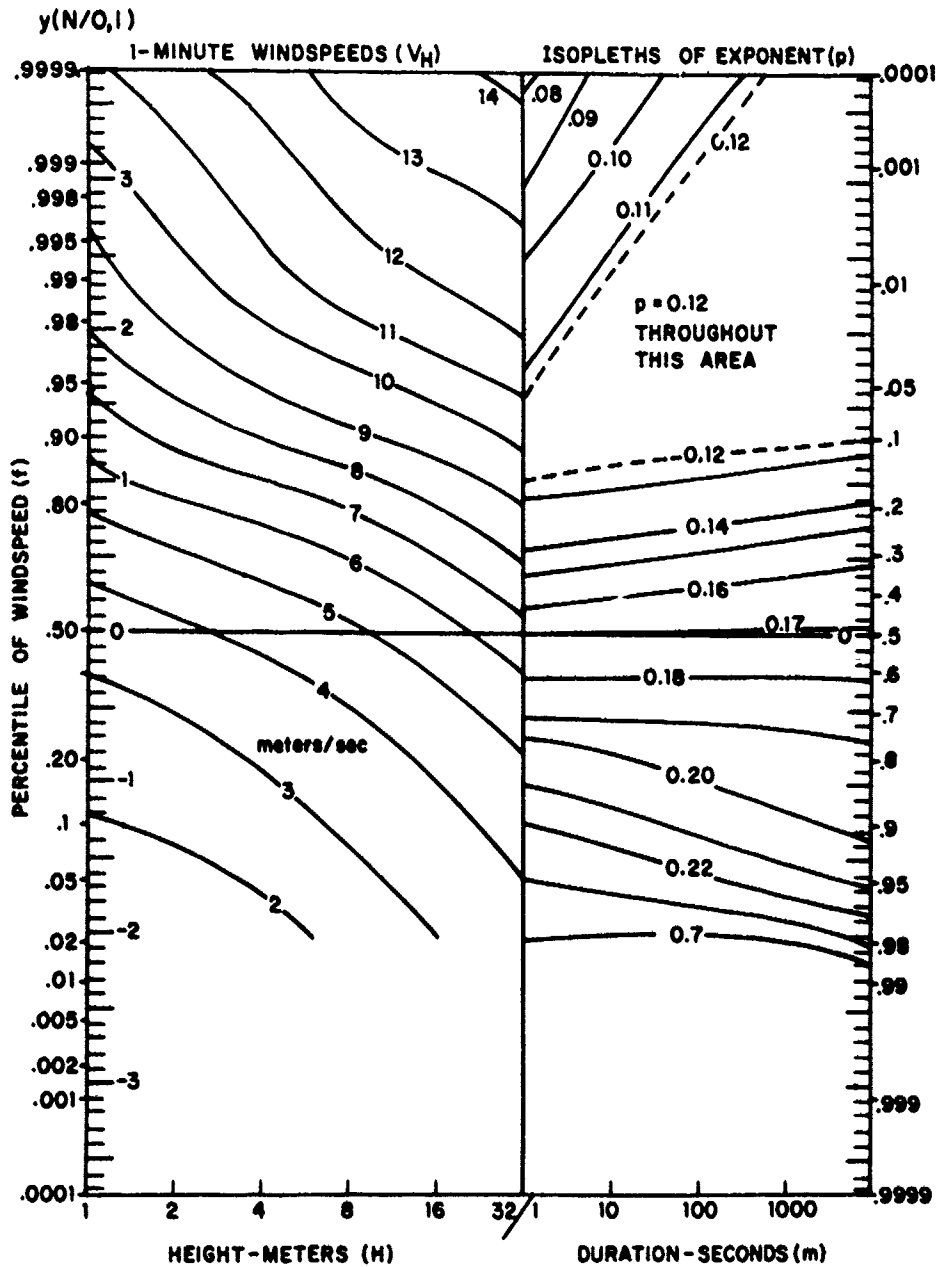


Figure 6.1. A Nomogram to Obtain Windspeeds of Duration 1 to 1000 Sec at a Height of 1 to 32 m (the right hand side of the Nomogram shows the exponent (p) in the wind power model [Eq. (6.2)] as a function of the duration of the wind, including 1-sec, 1-min, 5-min and 1-hr averages, and as a function of the strength of the wind (in percentiles). Left-hand side shows percentiles of 1-min windspeed as a function of height above ground level)

The validity of a wind extrapolation to another height is dependent on the representativeness of the wind measurement at the reference level. If the anemometer mast is in a poorly defined terrain, the use of the wind profile formula is questionable. Uniformity of the terrain would improve the result. Winds observed with a land-based anemometer cannot be used to estimate the wind speed over an adjacent water surface. In certain cases the wind speed over terrain may attain a maximum speed at a level significantly below 100 m. Such cases usually occur in cold air flow, for example nocturnal down-slope winds or sea breezes.

6.2.2 Wind Duration Shift (Below 3,000 meters)

Normally, wind direction changes with height. Changes in direction with height are termed veering if the wind turns clockwise and backing if the wind turns counter clockwise. Veering is usually expressed as the rate of turning in degree per height interval (negative for backing).

Wind direction shifts with height are caused by surface frictional effects, and by height changes of the horizontal pressure patterns controlling the mean airflow. The following discussion excludes such phenomena as slope winds, land and sea breezes, nocturnal low-level airflow conditions in the equatorial zone, and rapid, small-scale wind fluctuations.

In the free atmosphere, the mean horizontal airflow is a gradient wind, approximately parallel to the isobars, the lower pressure being to the left. Surface friction reduces the speed, causing a component of the surface wind to blow across the isobars toward lower pressure. Thus, the wind direction changes with height to align itself with the gradient wind in the free atmosphere.

To a first approximation, it can be said that under strong mean wind conditions in the Northern Hemisphere, the winds will veer with height in the lower 1000 m, the magnitude of the veering being determined by the intensity of thermal advection processes. Warm air advection increases veering, and cold air advection either decreases the magnitude of frictional veering or causes backing of the winds. The conditions for veering and backing are reversed in the Southern Hemisphere. North of approximately 20°N latitude, winds in the lowest 1000 m of the atmosphere will usually display varying degrees of veering with relatively few cases of backing. Southerly surface winds will veer more with height than northerly surface winds. Above approximately 1000 m, southerly winds will continue to veer with height, while northerly winds will begin to show backing with height.

Table 6.6, 6.7, and 6.8 indicate the order of magnitude of veering with associated general meteorological conditions. Because no advection is permitted for the situation described in Table 6.6, the veering with height is almost constant and represents the gradual decrease of the surface frictional effect with height. Once

the gradient level of the free atmosphere is reached, frictional effects and, hence, veering become negligible in the case of no advection. Strong surface winds generally make an angle with the gradient wind of 10° to 30°; this is the overall veering found in the frictional layer of the atmosphere when little or no advection exists. The direction of the surface wind is insignificant. Total veering over the entire layer of frictional influence depends primarily on the roughness characteristics of the earth surface. The average for oceans is 5° to 15°; for continents, 25° to 45°. The average veering is usually greater in winter than in summer, and greater at northern stations than at southern stations. The averaging process masks the variability of veering that would be encountered with isolated observations in time and space. In the first 1000 m of the atmosphere, however, the importance of the general direction of the surface wind in obtaining reasonable estimates of veering appears doubtful. Above this layer, southerly winds veer with height, northerly winds back with height. Maximum values of veering in the frictional layer are near 1°/100 m; isolated cases of backing of the order of magnitude are observed.

In summary, the average total veering (or backing) in the lower 1000 m is 20° to 40°, with isolated cases of 70° to 90°. To a first approximation, it may be assumed that this veering (or backing) is evenly distributed throughout the layer. Above this layer, primarily dependent on horizontal advection conditions, winds will show veering or backing with approximately the same average order of magnitude as in the frictional layer.

Table 6.6. Typical Frictional Veering of Wind Over Plain Land With Moderately Strong Gradient Winds (18 m/sec) and No Temperature Advection; 51.3°N, 12.5°E, 20 October 1931. (After H. Lettau, *Tellus*, Vol. 2, p 125, 1950)

Altitude (100 m)	Average Speed (m/sec)	Angle* (deg)	Veering (deg/100 m)
6.0 to 9.0	18	7	2.3
3.0 to 6.0	16	15	2.6
1.5 to 3.0	13	21	2.6
0.0 to 1.5	9	25	2.3

* Angle between wind and the gradient wind.

Table 6.7. Average Angle Formed by the Wind and the Gradient Wind, and Average Veering for Weather Stations in Germany, Grouped According to Topography. (After H. Lettau, *Atmosphärische Turbulenz*, Akademische Verlagsgesellschaft M. B. H., Leipzig, 1939)

Altitude (100 m)	Coastal Plains	Rolling Country	Hilly Land
ANGLE (deg)			
9.0 to 15.0	0	2	3
6.0 to 9.0	2	5	10
3.0 to 6.0	10	17	25
1.5 to 3.0	22	30	36
0.0 to 1.5	29	36	43
VEERING (deg/100 m)			
9.0 to 15.0	0.3	0.7	1.0
6.0 to 9.0	0.7	2.0	3.9
3.0 to 6.0	4.3	5.9	5.2
1.5 to 3.0	4.9	4.6	4.3
0.0 to 1.5	4.9	3.0	4.3

Table 6.8. Average Veering (deg/100 m) for Various Ranges of Height; Means (1918 to 1920) for Three Stations in U. S. A. in the Latitude Zone 31° to 36° (average 33°N), and Three in Latitude Zone 40° to 45° (average 43°N). (condensed from W. R. Gregg, *Monthly Weather Review*, Suppl. No. 20, 1922)

Altitude (100 m)	Southerly Surface Winds				Northerly Surface Winds			
	Summer		Winter		Summer		Winter	
	33°N	43°N	33°N	43°N	33°N	43°N	33°N	43°N
27.0 to 36.0		2.3	3.3	2.3		-3.3	-3.0	-2.3
15.0 to 27.0	1.0	3.3	2.3	3.3	-1.0	-3.3	-1.0	-2.3
6.0 to 15.0	1.0	2.3	2.3	3.0	-1.6	-1.3	-1.0	-2.3
3.6 to 6.0	3.0	2.3	3.3	3.3	-1.0	-1.0	3.0	3.0
1.5 to 3.6	2.3	2.3	3.0	4.3	2.3	2.3	3.0	4.3
0.0 to 1.5	2.3	2.3	3.6	4.3	1.6	2.3	3.6	4.3

6.2.3 Diurnal Variations and low-Level Jet Streams (Below 2,000 meters)

The mean diurnal variation of wind speed at various heights above any given site is caused by diurnal variations of both the horizontal pressure gradient force and the frictional force. The regular variations of the former are controlled by tidal effects (solar and lunar) which produce predominantly a 12-hourly wave, and by differential solar heating of the air over different locations and subsequent horizontal density gradients. In the troposphere the tidal motions of the atmosphere are small (range less than 0.5 mps). The barometric effects of differential solar heating produce marked diurnal wind variations only in special locations (along coast lines and the rims of extended high plateaus). Over most parts of the continents the diurnal variation of wind speed is controlled by the horizontally uniform effects of the cycle of solar heating and nocturnal cooling of the earth's surface. Consequent changes in the vertical thermal stratification of the atmosphere at 1000 to 2000 m significantly influence the effective frictional force in large-scale air flow.

Over relatively smooth land, the daytime thermal stratification intensifies the vertical mixing and the nocturnal thermal stratification weakens it. This causes a wind speed maximum near the ground at about mid-afternoon, and a minimum in the early morning hours. As seen in Figure 6.2, the phase of diurnal wind variation is reversed approximately 100 m above the ground, a level that varies with climatic zone, season, and surface roughness from 100 to 200 meters. The amplitude of the diurnal variation of wind speed normally has two maxima, at approximately 6 and 600 meters. The vertical extent of such diurnal variation varies roughly as the vertical extent of convective activity (2000 m).

Over the midwestern United States, the nocturnal maximum of wind speed above approximately 100 m frequently leads to a sharp peak of the velocity profile at heights of 300 to 900 meters. The peak, usually at the top of the nocturnal inversion, is significantly stronger (supergeostrophic) than explained by a balance between the horizontal pressure gradient and the Coriolis forces; it is often associated with extremely large values of wind shear. These peak winds are called low-level jet streams. The supergeostrophic wind speeds (peak speeds up to 26 mps in a pressure field resulting in 10 to 15 mps of geostrophic speed) suggest that an inertial oscillation of the air masses is induced when the constraint imposed by the daytime mixing is released by the initiation of stable thermal stratification near sunset. Average wind profiles showing the development of a low-level nocturnal jet stream over O'Neill, Nebraska, are given in Table 6.9 A particularly large value of wind speed variation with height, recorded during the development of a low-level

*This is based on the section by H. H. Lettau and D. A. Haugen in the Handbook of Geophysics for Air Force Designers, 1957.

jet stream, was obtained by kite observation at Drexel, Nebraska, on the night of 18 March 1918; the surface wind speed was 2.6 mps, but at an elevation of 238 m, the reported wind speed was 36 mps, yielding an average shear of 0.14 sec^{-1} .

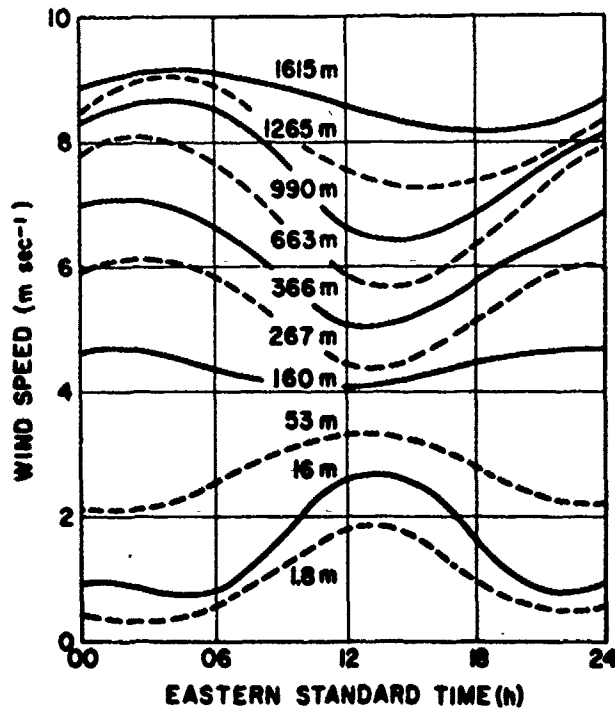


Figure 6.2. Diurnal Curves (slightly smoothed) of Annual Mean Wind Speed at Oak Ridge, Tennessee, Average for 1948 to 1952 (the wind speed data at heights of 1.8 and 16 m are from anemometer recordings; for other heights, data were obtained from pilot-balloon soundings at 4-hr intervals [dashes are for clarity of illustration].)

Over the ocean the diurnal variation of wind speed is negligible because diurnal variations in thermal stratifications are extremely small. In coastal regions where land and sea breezes are experienced, the amplitude and phase of the diurnal variation of wind speed are comparable with those over land. A reversal of phase with height is questionable, however. The vertical extent of the sea breeze is roughly 1000 m, the land breeze roughly 500 m, the over-all land-sea breeze system, including return flow, about 3000 m.

Table 6.9 Average Wind Profiles (Speed and Direction at Various Heights) Showing Development of Nocturnal Low-Level Jet Stream (Average of five nights of observations, Great Plains Turbulence Field Program, O'Neill, Nebraska)

Height (km)	Mean Local Time							
	1800		2000		2200		2400	
	Speed (m/sec)	Dir (deg)	Speed (m/sec)	Dir (deg)	Speed (m/sec)	Dir (deg)	Speed (m/sec)	Dir (deg)
2.0	6.1	223	4.3	225	3.5	223	3.1	231
1.8	7.2	219	5.0	226	4.0	227	3.4	233
1.5	9.4	213	8.3	225	5.6	229	5.0	232
1.2	10.9	207	12.3	217	10.8	225	8.9	223
0.9	11.6	194	14.7	202	13.9	211	13.1	219
0.8	11.7	190	15.5	193	15.9	204	16.2	213
0.6	11.6	182	15.8	190	17.2	196	19.6	203
0.5	11.5	180	15.6	185	17.9	190	20.1	196
0.3	10.8	177	14.7	178	18.0	183	18.9	189
0.2	9.7	174	13.6	171	14.9	175	15.1	183
0.1	9.2	173	12.2	167	12.8	170	12.9	170
Height (km)	0200		0400		0600		0800	
	Speed (m/sec)	Dir (deg)	Speed (m/sec)	Dir (deg)	Speed (m/sec)	Dir (deg)	Speed (m/sec)	Dir (deg)
	2.0	4.0	227	3.7	214	3.3	208	4.5
1.8	4.2	226	3.9	220	3.7	212	4.9	208
1.5	5.4	226	4.5	227	4.8	213	6.2	204
1.2	8.5	227	8.0	228	6.7	218	8.3	203
0.9	13.5	224	12.1	228	10.5	220	11.2	213
0.8	16.5	219	14.5	225	12.7	220	12.4	215
0.6	18.9	211	17.5	217	15.6	217	13.9	215
0.5	19.9	203	18.9	209	17.2	213	14.9	213
0.3	19.0	196	18.7	199	17.3	204	14.0	204
0.2	17.1	189	16.2	191	14.5	195	12.6	195
0.1	13.4	187	13.9	189	12.7	191	11.8	191

The various features of local wind variation discussed here occur quite frequently. In general, they are easily observable during conditions of clear skies and light to moderate intensity of the large-scale airflow. It should be remembered, however, that when the diurnal variations are not readily observable, it may be because they are superimposed on the large-scale airflow. Empirical wind structure models not accounting for possible diurnal variations could then be in error.

6.3 LARGE SCALE WIND STRUCTURE

This section provides information on the vertical and horizontal distribution of winds for altitudes up to 90 km. The wind data for altitudes up to about 26 km are based on routine rawinsonde observations taken by the National Weather Service. The root mean square (rms) observational errors in vector wind measurements using FPS-16, T-19, or similar tracking radar for altitudes up to 26 km are 1 m sec^{-1} plus 2 percent of the vector wind speed. The information presented on winds between 26 and 60 km was obtained from Meteorological Rocket Network (MRN) observations. Most of the available observations are for locations in the Northern Hemisphere. The estimated rms observational errors at these altitudes are 2 m sec^{-1} plus 3 percent of the vector wind. The wind distribution at altitudes between 60 and 90 km are based on data obtained from grenade and inflatable falling sphere experiments. The estimated rms error for the falling sphere observations, which make up the largest portions of the data, is to 2 to 3 m sec^{-1} between 60 and 90 km.

6.3.1 Seasonal and Day-to-Day Variations

The broad features of the seasonal change in winds between the surface and 90 km are reasonably well established. Figure 6.3 is a meridional cross section of the observed mean monthly zonal wind components for January and July from the surface to 80 km. The seasonal change in the stratospheric and mesospheric wind fields differs from tropospheric seasons in timing and length of season. At middle and high latitudes long periods of easterly and westerly flow are separated by shorter periods of transition as shown by the curves of the mean monthly 50-km zonal wind components in Figure 6.4 for White Sands, 32° N , Wallops Island, 38° N , and Fort Churchill, 59° N . The mean monthly meridional components (Figure 6.4) are less variable and maintain a slight southerly (positive) component at most locations throughout the year.

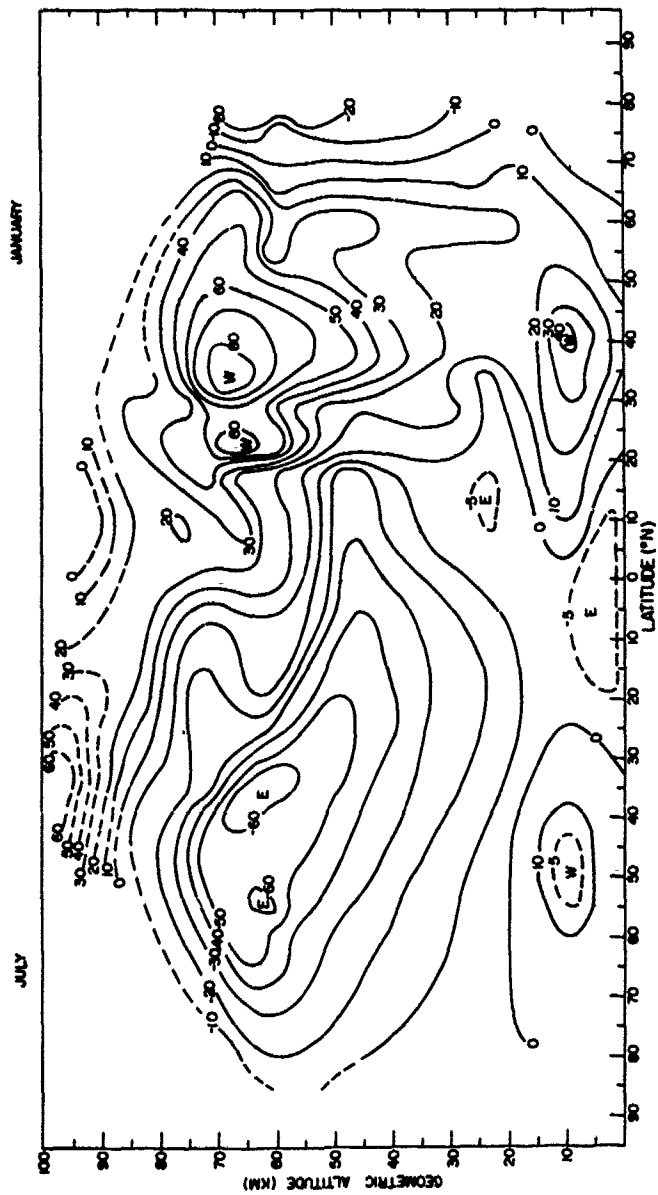


Figure 6.3. Meridional Cross Section of Zonal Wind Speed (m/sec)

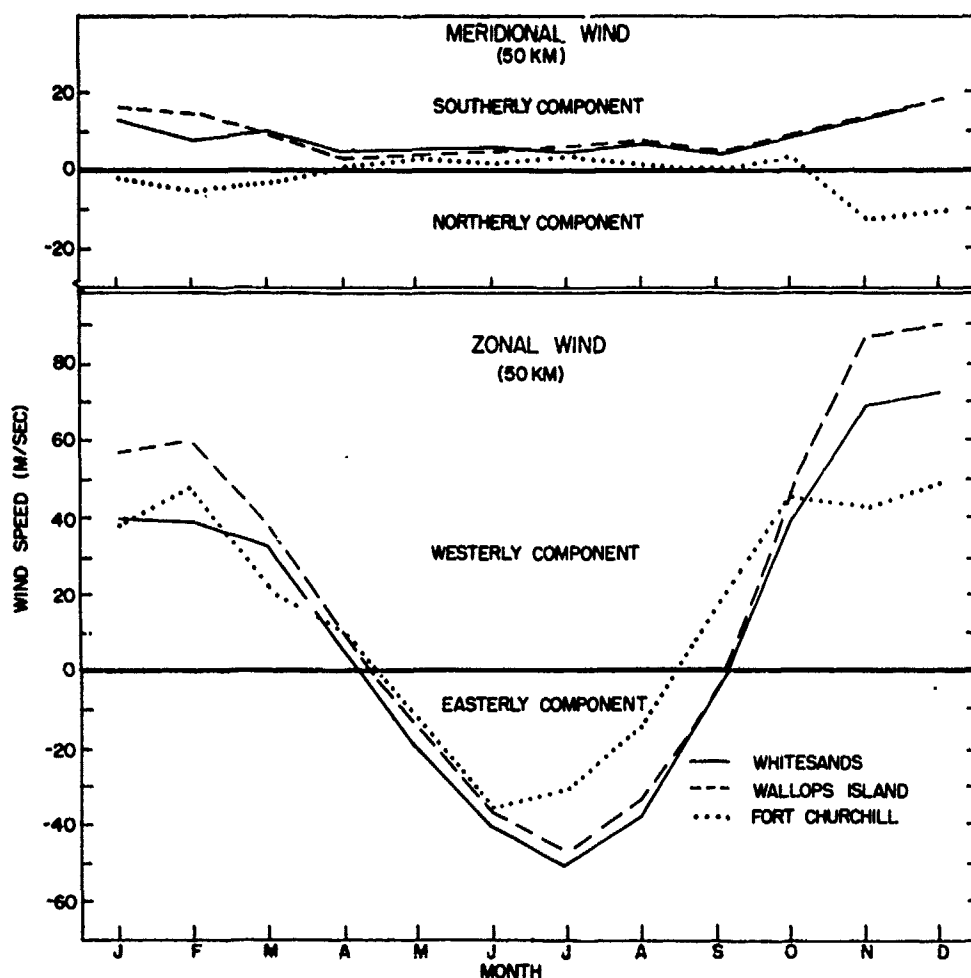


Figure 6.4. Annual Variation of Meridional and Zonal Wind at White Sands, Wallops Island and Fort Churchill

Profiles of mean monthly zonal wind speeds (m sec^{-1}) for each of the midseason months at Ascension Island, Wallops Island and Churchill, from a report by Kantor and Cole⁶ are plotted in Figure 6.5 for altitudes up to 60 km. The seasonal variations in the mean monthly zonal winds are largest at Wallops Island, a midlatitude location, and at altitudes above 30 km. The largest day-to-day variations around the mean monthly values (Figure 6.6) occur during the winter months at altitudes above 20 km at middle and high latitudes.

6. Kantor, A. J., and Cole, A. E. (1980) Wind Distributions and Interlevel Correlations, Surface to 60 km, ERP No. 713, AFGL-TR-80-0242, AD A092670.

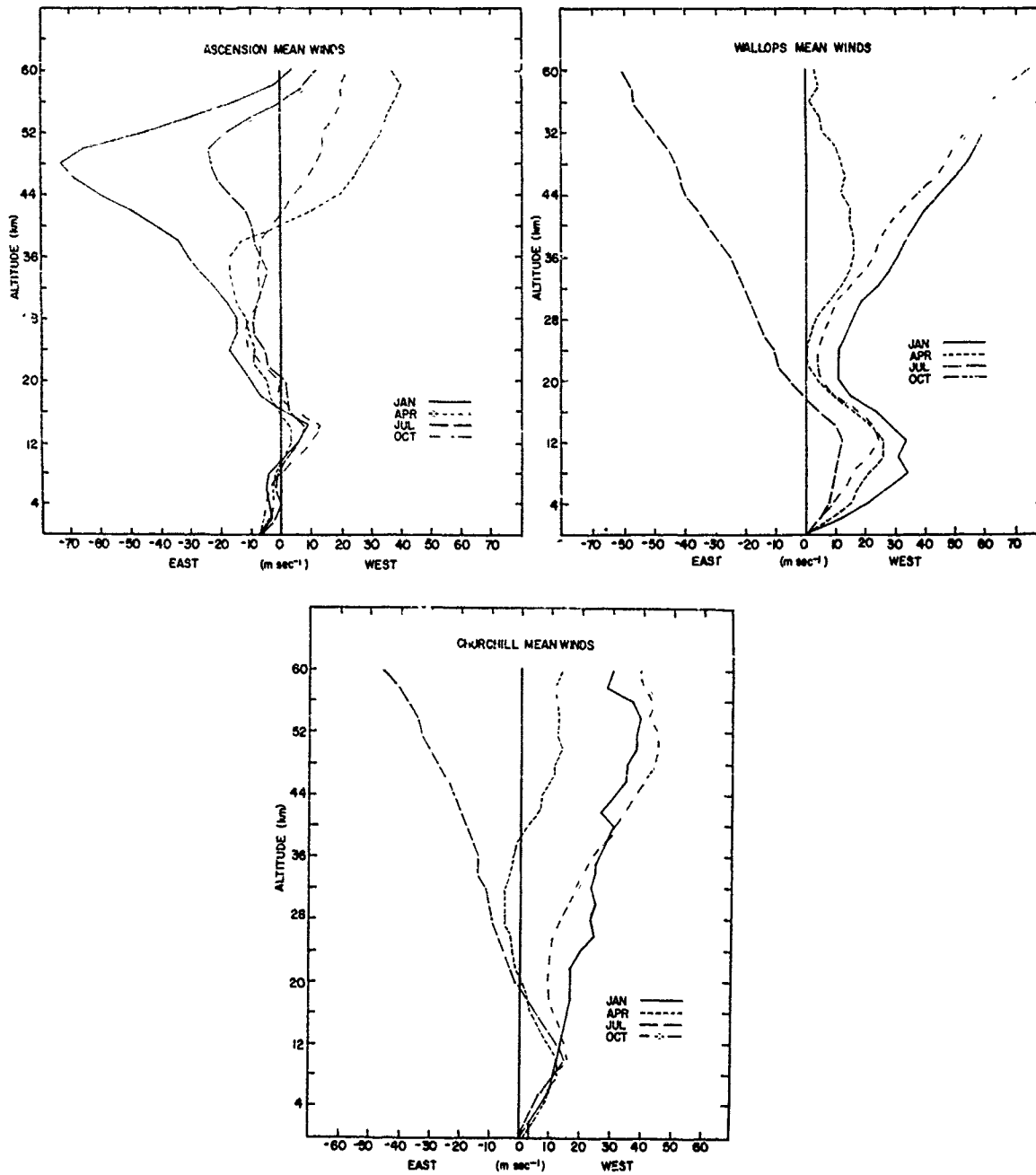


Figure 6.5a. Seasonal Effects on the Zonal Wind Profiles at Ascension Island, Wallops Island and Churchill

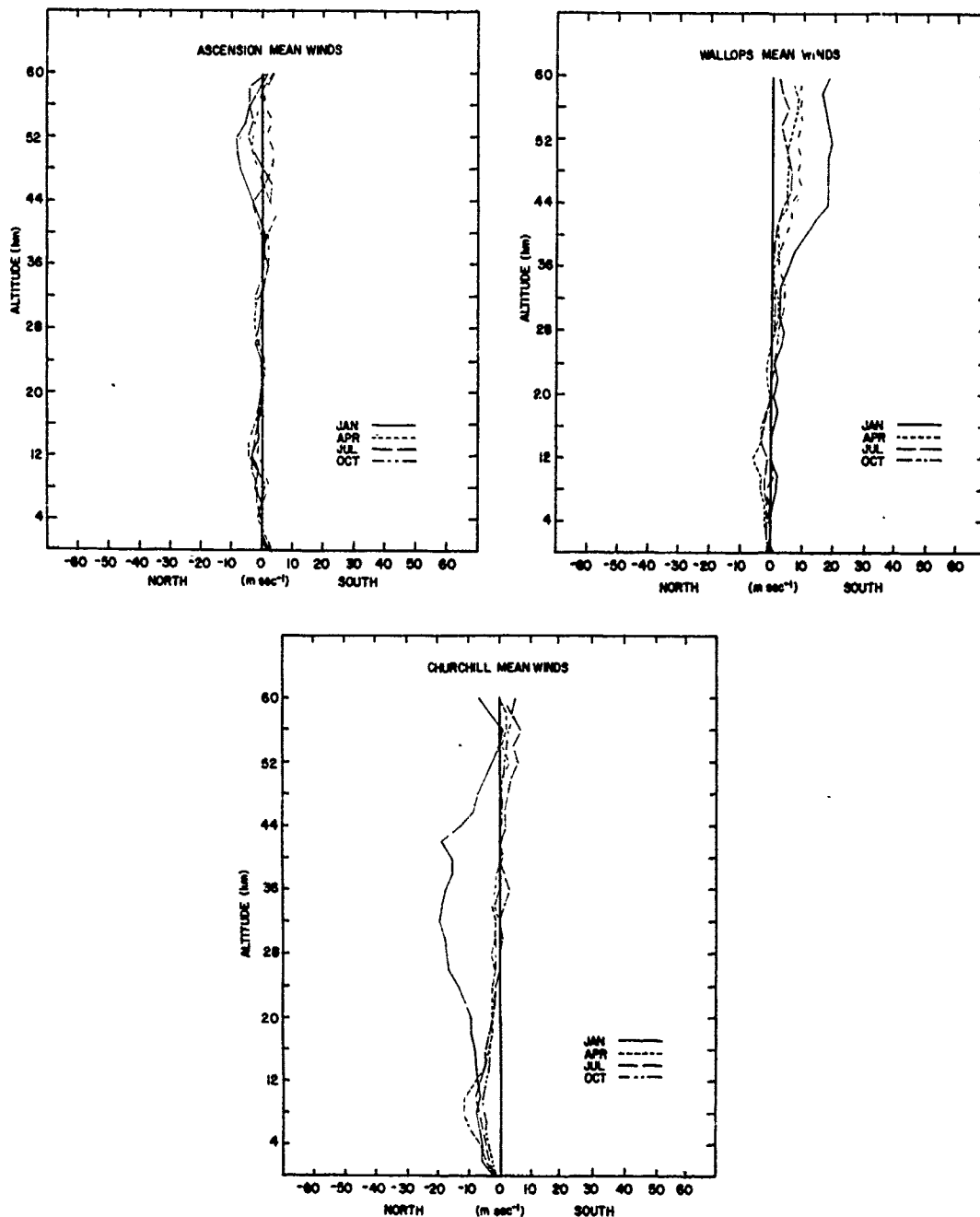


Figure 6.5b. Seasonal Effects on the Meridional Wind Profiles at Ascension Island, Wallops Island and Churchill

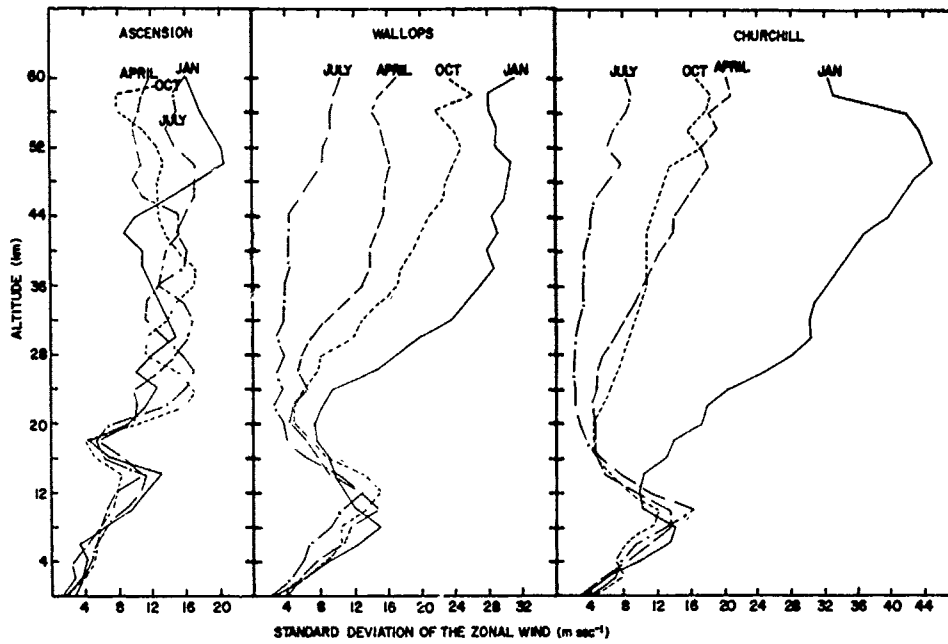


Figure 6.6a. Day-to-Day Variability Around Mean Monthly Zonal Winds for the Midseason Months at Ascension Island, Wallops Island and Churchill

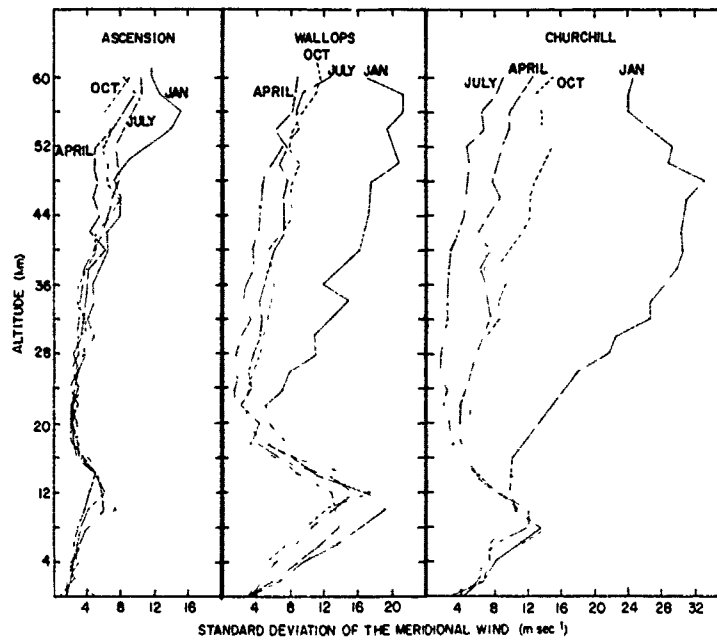


Figure 6.6b. Day-to-Day Variability Around Mean Monthly Meridional Winds for the Midseason Months at Ascension Island, Wallops Island and Churchill

6.3.2 Time and Space Variations

The change and movement of pressure patterns in the atmosphere cause standard wind observations (for example, the mean wind over 1 min) to vary from time to time at a given place, and from place to place at a given time. In general, as shown in Figure 6.7, the amount of change in wind between two observations increases with the time interval between them and with the distance between observing points. The rate of increase in wind change with increasing time or space interval between observations is, in turn, a variable depending upon season, geographic location, average wind speed, nature of the sample, and, to some extent, height above the ground.

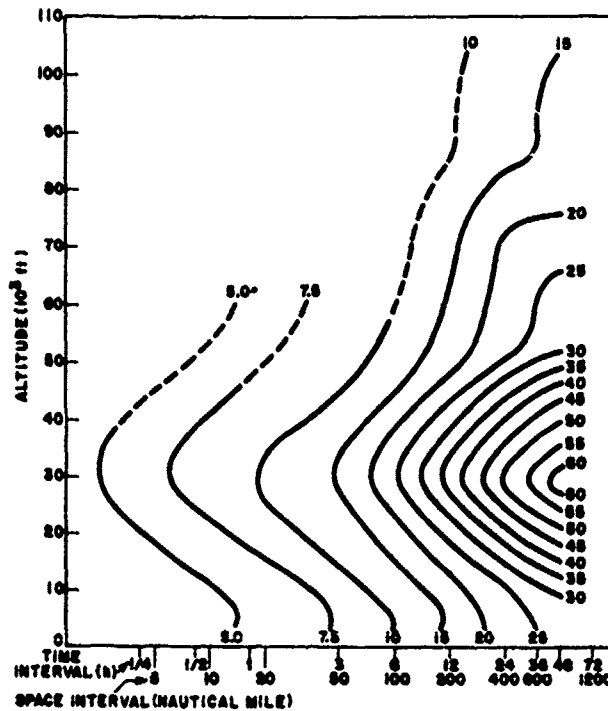


Figure 6.7. Isopleths of Time and Space Variabilities of Changes in the Mean Vector Wind With Altitude; the rms (63rd percentile) Values, in Knots, of Observed Changes for Various Time Lags Between Observations, and of Derived Changes for Various Distances are Given on Each Curve [from Ellsaesser¹²]

Most of the wind variability data pertaining to the free atmosphere below 30 km are derived from standard pilot balloon or rawinsonde observations. Lower limits of resolution of these observations are such that minimum intervals for wind variability are about 15 min or 6 km. The small-scale fluctuations appear to be fairly random, and their combined effect on ballistic or synoptic-scale forecasting problems normally cancel out and, thus, are neglected.

Observations of VHF and UHF radar backscatter from turbulence in the clear atmosphere, conducted at several locations during the past several years, permit much more detailed measurement of the time variation of vector winds than was previously attainable. Depending on the radar wavelength and the power-aperture product (Gage and Balsley⁷); measurements are obtainable from near the surface to about 100-km altitude. Several radars which were originally designed for ionospheric research have been used for observations of the neutral (non-ionized) atmosphere, and a few radars have been built specifically for tropospheric and stratospheric wind measurements. The latter include NOAA radars in Colorado and Alaska and the SOUSY-VHF-Radar operated by the Max-Planck-Institute für Aeronomie in the Federal Republic of Germany. Examples of data are presented by Green et al,⁸ Balsley and Gage,⁹ Röttger,¹⁰ and in numerous other publications. A radar of this type has been incorporated into the NOAA Prototype Regional Observation and Forecasting System (PROFS).

Several measures of wind variability are possible. The most useful measure is the rms of the vector change in wind; others commonly used are the mean and the median absolute vector differences. All of these are scalar measures computed from the magnitudes of the difference vectors. They are related in a circular normal distribution which is usually a good approximation to the frequency distribution of wind changes.

6.3.2.1 TIME VARIABILITY UP TO 30 km

The time rate of change of wind in the frictional layer is affected by the topography and the thermal structure. The results in Table 6.10 are for steady southerly flow conditions from seven observational periods, all but one of which extended

7. Gage, K.S., and Balsley, B.B. (1978) Doppler radar probing of the clear atmosphere, Bull. Amer. Meteor. Soc. 59:1074-1092.
8. Green, J.L., Gage, K.S., and Van Zandt, T.E. (1979) Atmospheric measurements by VHF pulsed Doppler radar, IEEE Trans. Geosci. Electr. GE-17:262-280.
9. Balsley, B.B., and Gage, K.S. (1980) The MST radar technique: Potential for middle atmospheric studies, Pure and Appl. Geophys. 118:452-493.
10. Röttger, J. (1979) VHF radar observations of a frontal passage, J. Appl. Meteor. 18:85-91.

over 24 hr (pilot balloon, rawinsonde, and smoke-puff observations are combined). The effect of thermal stratification is indicated by comparison of the day and night values for time differences up to 8 hr.

Table 6. 10. Mean and Standard Deviation of Absolute Value of Vector Velocity Differences at Various Time Intervals, Δt , in the Lower 1829 m (600 ft) Over Smooth Open Terrain (Great Plains Turbulence Field Program)

Height (1000 m)	Velocity Differences (m/sec)							
	$\Delta t = 2$ hours		$\Delta t = 4$ hours		$\Delta t = 8$ hours			
1.8	3.0 ± 1.7	3.3 ± 2.4	5.0 ± 2.6	4.5 ± 3.2	7.4 ± 2.4	4.0 ± 2.9		
1.4	2.6 ± 1.5	2.8 ± 1.9	4.2 ± 2.5	4.2 ± 2.6	5.4 ± 2.8	5.1 ± 3.3		
0.9	2.6 ± 1.7	3.9 ± 2.5	4.1 ± 2.2	5.6 ± 2.6	5.4 ± 1.9	7.5 ± 3.1		
0.5	3.1 ± 2.2	4.0 ± 2.8	4.8 ± 3.1	6.5 ± 3.5	6.8 ± 2.8	9.6 ± 3.1		
0.4	3.0 ± 1.9	4.0 ± 3.0	4.8 ± 3.1	6.9 ± 4.5	7.1 ± 3.5	6.2 ± 3.5		
0.2	2.6 ± 2.4	3.4 ± 3.1	4.3 ± 2.9	6.0 ± 5.4	6.2 ± 3.1	8.9 ± 4.9		
	$\Delta t = 12$ hours		$\Delta t = 16$ hours		$\Delta t = 20$ hours		$\Delta t = 24$ hours	
1.8	5.6 ± 2.9		6.4 ± 3.1		7.5 ± 3.5		6.5 ± 3.3	
1.4	6.3 ± 3.1		6.6 ± 3.0		5.9 ± 2.1		4.8 ± 2.6	
0.9	7.8 ± 3.9		7.7 ± 3.5		5.9 ± 2.8		4.4 ± 2.6	
0.5	10.2 ± 3.9		8.8 ± 4.1		6.9 ± 4.0		4.9 ± 3.3	
0.4	10.4 ± 4.1		8.8 ± 3.6		7.1 ± 4.9		4.6 ± 2.9	
0.2	8.3 ± 3.7		7.2 ± 3.8		6.0 ± 4.9		4.3 ± 3.9	

The change in wind variability above the frictional layer with increasing time between observations and with altitude is illustrated in Figure 6.7. Figure 6.8 shows the effect of latitude and season for a 24-hr lag between wind observations.

For relatively short periods during which the pattern of the winds is fairly stable, the variability of the wind is given directly by

$$S_t = Kt^p, \quad (6.3)$$

where S_t is the rms change in wind during the time interval t , and K is a constant. The exponent p depends on r_t , the correlation coefficient between winds separated by the time interval t . At short lags where r_t is 1, p is 1; at greater lags where r_t is 0, p is 0.5. For t in hours and S_t in miles per hour,

$$S_t = 4 t^{0.5} \quad (6.4)$$

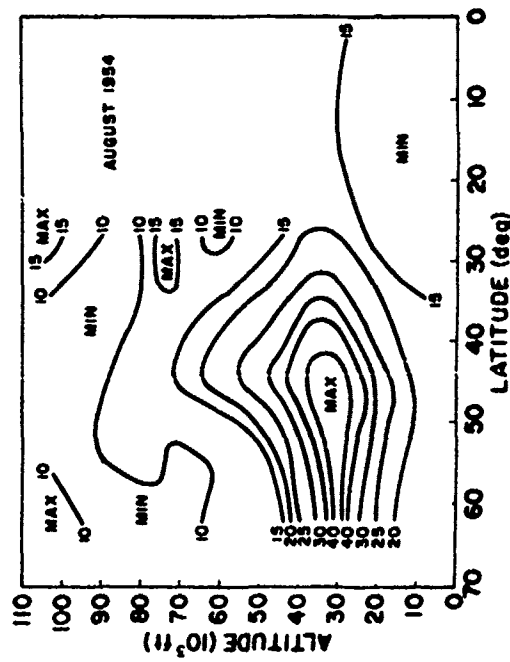
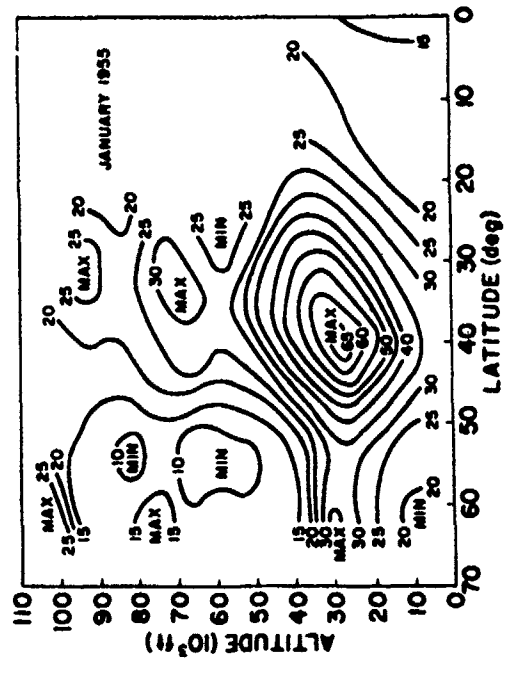


Figure 6. 8. Distribution in Latitude and Altitude of the Vector Wind Variability (St) for a 24-hr Time Lag Between Observations Along the Meridian 75° W in Summer and Winter (August 1954 data are for East Africa); rms Values in Knots are Shown on Curves [from Ellsasser (1960)]

is a suitable generalization for middle latitudes and for lag intervals of 30 min to about 12 hours. Although this empirical relation is an acceptable average, K actually depends on the mean wind speed. The mean wind varies with season, altitude, and geographic location (see Figure 6.5); hence, values of K other than 4 will, on some occasions, be more applicable to engineering problems. Values of K from 3.4 to 14.2 are tabulated by Arnold and Bellucci.¹¹ An analysis of the relationship of K to the mean wind in a stable flow pattern shows that K increases from about 1 at speeds of 5 mile hr^{-1} to perhaps 5 or 6 at speeds of 35 mile hr^{-1} and higher.

An indirect model relates the variability in time to r_t and to the climatological dispersion of the winds. This relationship is given by

$$S_t = \sigma_t \sqrt{2(1 - r_t)}, \quad (6.5)$$

where σ_t is the standard vector deviation of the winds (rms deviation from the vector resultant wind). The vector stretch correlation coefficient between the initial wind having components u and v and the wind after a time interval t , having components x and y , is given by

$$r_t = \frac{\Sigma(ux + vy)}{\sqrt{\Sigma(u^2 + v^2) \Sigma(x^2 + y^2)}}. \quad (6.6)$$

This parameter undergoes an exponential decay with increasing lag, for intervals up to 24 hr or more, and then appears to oscillate about zero. The relation,

$$r_t = \exp(-0.0248t), \quad (6.7)$$

with t in hours, is widely used. This equation, in conjunction with Eq. (6.5) and values of α_t allows an estimate of the wind variability for a desired lag interval that pertains specifically to the place, season, and altitude of interest. This model has two serious limitations; it will not permit r_t to become negative, nor does the constant coefficient of t allow for variations in the rate of decay of the correlation. At sufficiently large time intervals, r_t does not become negative, and r_t is so close to zero for lags in excess of 72 hr that the model becomes unreliable. In some cases r_t becomes negative at shorter lags, and the lag at which this occurs varies from place to place. Investigations of the rate of decay of correlation show that it

11. Arnold, A., and Bellucci, R. (1957) Variability of Ballistic Meteorological Parameters, Tech. Memo. No. M-1913, Ft. Monmouth, N.J., U.S. Army Sig. Eng. Lab.

varies geographically, seasonally, and probably with altitude. The variation has been mapped only for the United States at 18,000 ft [Elsaesser¹²].

Attempts to develop a more precise model of the variability of winds with time have resulted either in only moderate improvement or extremely complex models. Thus Eq. (6.7) is considered the most useful approximation. When precision in estimating the wind variability with time is required, a special climatological study must be made.

6.3.2.2 SPATIAL VARIABILITY UP TO 30 km

In general, variability increases with increasing distance between observation points, and the rate of increase with distance depends on geographic location, season, and altitude. A change in the wind with time can be thought of as resulting in part from the movement of wind-field patterns over the observing point, and thus as analogous to the spacial variability.

Extending this analogy to the models, the space variability of wind S_d , is given by $K'd^p$, where d is the distance between observing points. The parameter K' varies with season, geographic location, and altitude, but no detailed examination has been made of the way in which these factors act. Arnold and Bellucci¹¹ tabulated values of K' from 1.1 to 6.1. They consider the expression,

$$S_d = 1.5d^{0.5}, \quad (6.8)$$

where S_d is in miles hr^{-1} and d in miles, as representative for middle latitudes.

The indirect model provides several empirical curves for the decay of the correlation coefficient of winds with increasing separation between observing points. These curves indicate differing rates of decay depending upon latitude and upon the orientation of the line connecting the observing points. The analogy between time and space variability of the winds extends to these curves. Figure 6.7 indicates that, for temperate latitudes, a general approximation to the space variability of winds can be obtained by taking 3 hr as equivalent to 30 nautical miles. The space variability is then estimated in a manner similar to time variability from $\sigma_d \sqrt{2(1 - r_d)}$; where r_d is the correlation coefficient between winds separated by the distance interval d .

6.3.2.3 TIME AND SPACE VARIATIONS - 30 to 60 km

Observations show that pronounced diurnal and semi-diurnal oscillations exist in the winds at altitudes above 30 km. Sufficient data, however, are not available

12. Elsaesser, H. W. (1960) Wind Variability, AWS Tech. Rept. No. 105-2, Hdqts. Air Weather Service, Scott AFB, Illinois.

to permit the development of a satisfactory model for all latitudes and seasons. The results of an analysis of a series of wind observations taken at Wallops Island during a 48-hr period in May 1977, shown in Figure 6.9, provide an indication of the magnitude of the diurnal oscillation at a mid-latitude location. The X's in Figure 6.9 are average values of the north-south and east-west wind components at the indicated local times. The curves are based on a harmonic analysis of the meridional (N-S) and zonal (E-W) wind components. The amplitude of the combined diurnal and semi-diurnal oscillations of the N-S component, increases with altitude above 30 km, reaching a maximum of 10 to 11 m/sec between 50 and 55 km. The diurnal variations of the E-W component are not as well defined at 40 and 45 km. At altitudes of 50 km and above, however, the E-W amplitudes are between 12 and 14 m/sec. The magnitude of the diurnal oscillations are somewhat smaller in tropical and arctic regions.

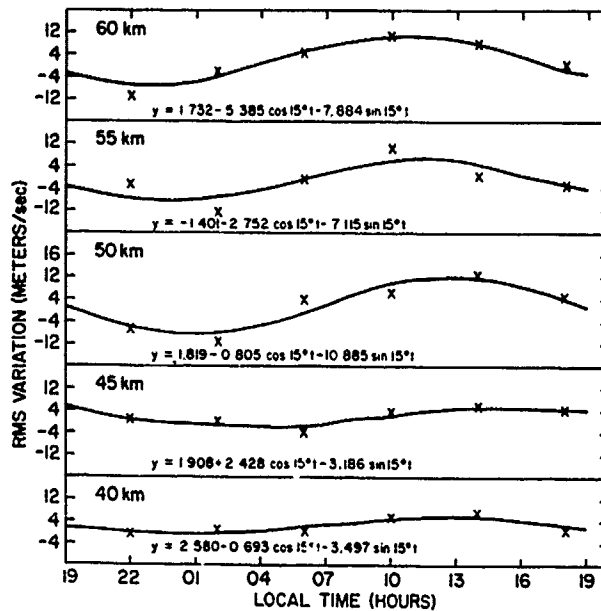


Figure 6.9a. Diurnal Wind Variations at Wallops Island in May (N-S)

Rms differences between wind components observed from 1 to 72 hr apart have been analyzed at altitudes between 30 and 60 km to obtain estimates of the variations in these components with time. Rms differences between the N-S wind

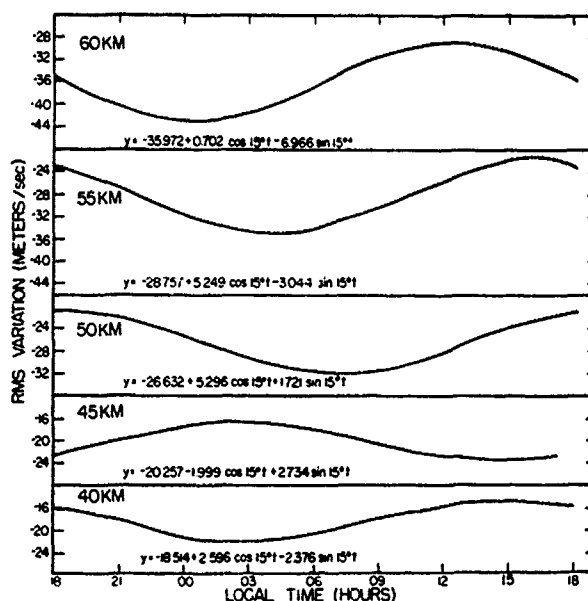


Figure 6.9b. Diurnal Wind Variations at Wallops Island in May (E-W)

components observed from 1 to 72 hr apart at Ascension, Ft. Sherman, and Kwajalein are shown in Figure 6. 10. Data for all seasons for these three stations have been combined. The values display a relatively stable rms variation of roughly 10 to 12 m/sec for periods up to 72 hr at 55 and 60 km and about 6 or 7 m/sec at altitudes of 40 and 45 km. There is an indication of the diurnal cycle with an amplitude of 1 to 2 m/sec at these altitudes as shown by the 24-hr harmonic curves which have been fitted to the individual values. Most of the observed variability can be attributed to random measurement errors as there is little difference in the rms variations between observations taken 6 hr apart and those taken 72 hr apart.

In summer, conditions are approximately the same at all latitudes, with little change in rms values with time. In winter, however, the rate at which the rms values increase with time varies with latitude. The larger day-to-day changes in the synoptic patterns at middle and high latitudes are reflected in well defined increases in the rms variability with time. At 50 km, for example, rms values for the N-S components at White Sands Missile Range (32° N) increase with time from 6 to 8 m/sec to 16 or 18 m/sec in 72 hr. At Poker Flats (64° N) and Churchill (59° N) they increase from 6 or 8 m/sec to 25 m/sec. The diurnal cycle in observed data is masked by the synoptic changes and instrumentation errors during the winter months at middle and high latitudes.

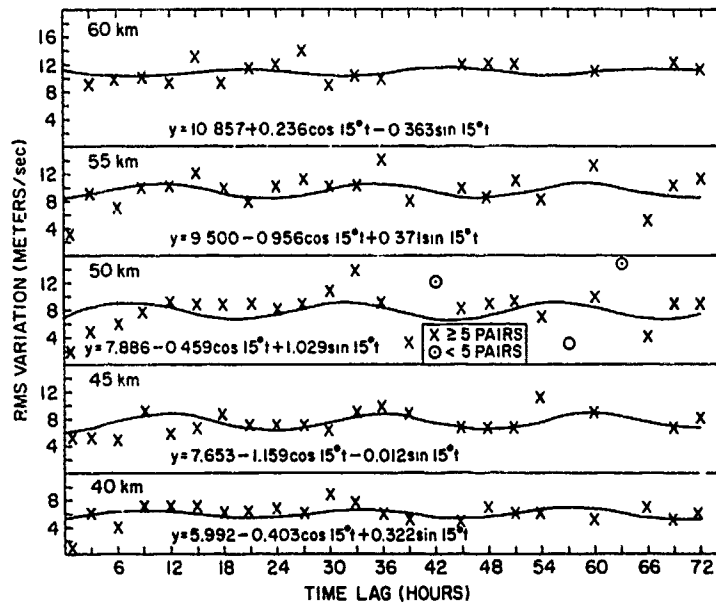


Figure 6.10. Rms Differences Between North-South Winds Observed 1 to 72 hr Apart in the Tropics

6.4 WIND PROFILES

6.4.1 Wind Shear

Wind shear is the derivative of the wind vector with respect to distance and is itself a vector. The shear of the horizontal wind is of primary interest and is the one discussed in this section. The terms vertical wind shear and horizontal wind shear are commonly used in referring to the shear of the horizontal wind in the vertical and horizontal directions, respectively. Horizontal wind shear is the derivative of the horizontal wind with respect to an axis parallel to the earth's surface. Its applications are restricted largely to meteorological analysis. Vertical wind shear is expressed as $\Delta W / \Delta y$, where ΔW is the change of the horizontal wind in the altitude interval Δy ; the unit of shear is sec^{-1} . Although direction is also necessary to specify the shear vector, it is usually ignored; for design purposes shear is normally applied in the most adverse possible direction.

The climatology of vertical wind shear is applicable to problems dealing with design and launch of vertically rising vehicles and jet aircraft, radioactive fallout investigations, and many phases of high-altitude research. Most investigations of shear climatology are for specific locations in order to satisfy design and operational requirements of missiles and other vehicles at or near launch sites. For

vehicles with other than a vertical flight path, vertical wind shear can be determined by multiplying the shear by the cosine of the angle between the vertical axis and the vehicle trajectory.

Measurements of vertical wind shear indicate that average shear behaves inversely with layer thickness (scale-of-distance). This is illustrated in Figure 6.11, which is based on a relatively large number of observations during the windiest months over Cape Canaveral, Florida. Figure 6.12, based on the same data, shows the variation of shear with altitude and with layer thickness; it provides, as an example, the vertical wind shear spectrum at Cape Canaveral with a 1 percent probability of occurrence.

Wind shears for scales-of-distance $\Delta y \geq 1000$ m in thickness are computed directly from radiosonde and rocketsonde observations, whereas smaller scale shears can be calculated directly only from special fine-scale observations. However, shears associated with scales-of-distance $\Delta y < 1000$ m can be estimated from the following relationship:¹³

$$\Delta u = \Delta u_{1000} \left(\frac{\Delta y}{1000} \right)^{0.7}, \quad (6.9)$$

where Δu is the shear, Δu_{1000} is the 1000-m shear, and Δy is the scale-of-distance in meters for thicknesses < 1000 meters.

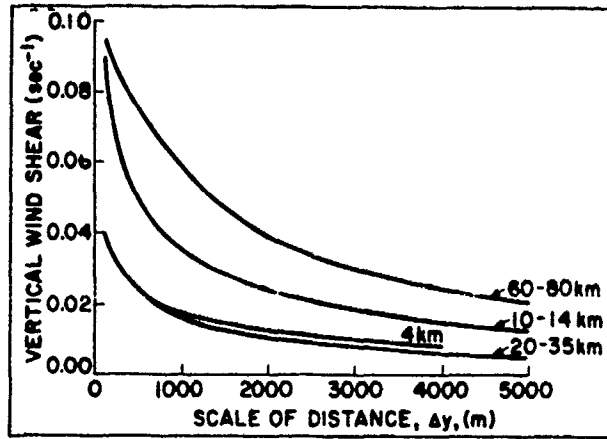


Figure 6.11. Selected Vertical Wind Shear Spectrums (4-, 10-, to -14, 20- to 35-, and 60- to 80-km Altitude) for Use With 5 Percent and 1 Percent Probability Level Wind Profile Envelope, Cape Kennedy, Florida [from Scoggins and Vaughan (1962)]

13. Fichtl, G.H. (1972) Small-scale wind shear definition for aerospace vehicle design, Jour. of Spacecraft and Rockets 9:79.

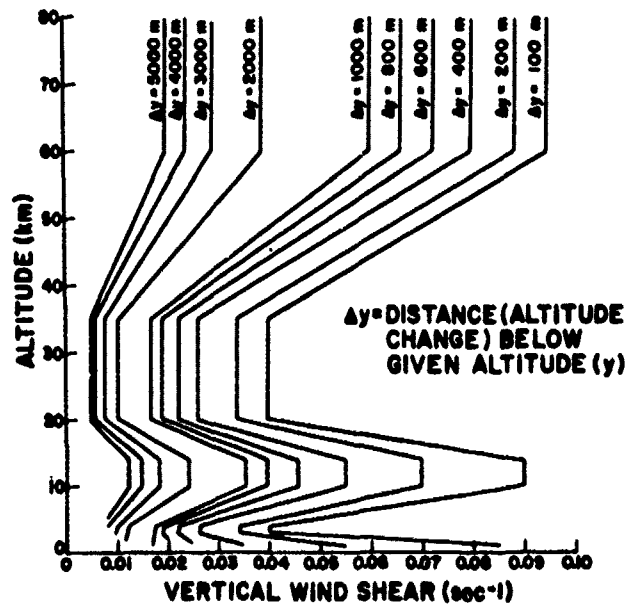


Figure 6.12. One Percent Probability-of-Occurrence Vertical Wind Shear Spectrum as Function of Altitude and Scale-of-Distance for Association With the 5 Percent and 1 Percent Wind Speed Profile Envelope for Cape Kennedy, Florida [from Scoggins and Vaughan (1962)]

Wind shear statistics for various locations differ primarily because of prevailing meteorological conditions, orographic features, and data sample size. As a result, significant differences exist in the shear structure for different locations. Consistent shear data for five vehicle launch and/or landing sites are presented in Tables 6.11 through 6.15 for the Eastern Test Range, Florida; Vandenberg AFB, California; Wallops Island, Virginia; White Sands Missile Range, New Mexico; and Edwards AFB, California. To get actual shear (sec^{-1}) from the indicated wind speed changes, divide by the appropriate scale-of-distance. Table 6.16 gives envelopes of the 99 percentile wind speed change for the five locations combined. The data contained in Table 6.16 are applicable when design or operational capability is not restricted to a specific launch site or may involve several geographical locations. Equation (6.9) was used to construct Tables 6.11 through 6.16¹⁴ for scales-of-distance < 1000 meters.

14. Kaufman, J. W. (Ed.) (1977) Terrestrial Environment (Climatic) Criteria Guidelines for Use in Aerospace Vehicle Design, NASA Technical Memorandum 78118, MSFC.

Table 6.11. Envelopes of 99 Percentile Wind Speed Change (m/sec), 1- to 80-km Altitude Region, Eastern Test Range (From Kaufman¹⁴)

Scales of Distance (m) Thickness										
Wind Speed at Reference Altitude (m/sec)	5000	4000	3000	2000	1000	800	600	400	200	100
≥ 90	77.5	74.4	68.0	59.3	42.6	36.4	29.7	22.4	13.8	8.5
= 80	71.0	68.0	63.8	56.0	40.5	34.7	28.5	21.4	13.2	8.1
= 70	63.5	61.0	57.9	52.0	38.8	33.1	27.0	20.3	12.5	7.7
= 60	56.0	54.7	52.3	47.4	36.0	31.0	25.3	18.9	11.7	7.2
= 50	47.5	47.0	46.2	43.8	33.0	28.3	23.2	17.5	10.7	6.6
= 40	39.0	38.0	37.0	35.3	29.5	25.3	20.6	15.5	9.6	5.9
= 30	30.0	30.0	29.4	26.9	22.6	19.4	15.8	11.9	7.3	4.5
= 20	18.0	17.5	16.7	15.8	14.6	12.5	10.2	7.5	4.7	2.9

Table 6.12. Envelopes of 99 Percentile Wind Speed Change (m/sec) 1- to 80-km Altitude Region, Vandenberg, AFB (From Kaufman¹⁴)

Scales of Distance (m) Thickness										
Wind Speed Reference Altitude (m/sec)	5000	4000	3000	2000	1000	800	600	400	200	100
≥ 90	66.9	62.5	57.8	51.5	37.5	32.1	26.1	19.7	12.0	7.4
= 80	64.1	60.8	56.6	48.8	36.9	31.5	25.6	19.1	11.6	6.8
= 70	62.0	59.2	54.8	48.1	36.0	31.0	25.0	18.6	11.2	6.5
= 60	57.1	54.5	51.3	45.4	32.7	28.5	23.0	17.1	10.2	5.3
= 50	49.6	47.8	45.7	42.1	30.1	25.9	21.8	15.6	9.2	5.0
= 40	39.4	38.8	37.9	35.5	25.9	23.5	19.6	14.9	8.8	4.8
= 30	30.0	29.4	28.3	26.3	20.5	18.6	15.8	12.2	8.0	4.6
= 20	20.0	19.8	19.5	18.4	15.0	13.1	10.9	9.0	6.3	4.3

Table 6.13. Envelopes of 99 Percentile Wind Speed Change (m/sec), 1- to 80-km Altitude Region, Wallops Island (From Kaufman¹⁴)

Scales of Distance (m) Thickness										
Wind Speed at Reference Altitude (m/sec)	5000	4000	3000	2000	1000	800	600	400	200	100
≥ 90	72.5	67.0	60.2	50.5	37.6	32.3	26.3	19.8	12.2	7.5
= 80	66.5	62.5	57.5	48.8	37.0	31.7	25.9	19.5	12.0	7.4
= 70	61.2	58.5	53.8	46.5	35.8	30.7	25.1	18.9	11.6	7.1
= 60	54.5	52.5	50.0	44.4	34.5	29.6	24.2	18.2	11.2	6.9
= 50	46.2	44.2	42.3	38.8	33.0	28.3	23.2	17.4	10.7	6.6
= 40	36.7	35.6	34.5	32.3	27.6	23.7	19.3	14.5	8.9	5.5
= 30	27.2	26.3	25.3	24.2	20.6	17.7	14.7	10.8	6.7	4.1
= 20	17.8	17.3	16.8	16.4	15.2	13.0	10.6	8.0	4.9	3.0

Table 6.14. Envelopes of 99 Percentile Wind Speed Change (m/sec), 1- to 80-km Altitude Region, White Sands Missile Range (From Kaufman¹⁴)

Scales of Distance (m) Thickness										
Wind Speed at Reference Altitude (m/sec)	5000	4000	3000	2000	1000	800	600	400	200	100
≥ 90	70.7	67.0	61.2	52.4	42.0	36.0	29.4	22.1	13.6	8.4
= 80	66.0	63.0	57.7	50.0	40.2	34.5	28.1	21.2	13.0	8.0
= 70	60.2	57.0	53.0	46.5	38.0	32.6	26.6	20.0	12.3	7.6
= 60	52.6	50.0	46.5	42.3	35.5	30.5	24.9	18.7	11.5	7.1
= 50	45.0	43.0	40.2	37.0	32.0	28.3	23.1	17.4	10.7	6.6
= 40	36.5	35.5	34.8	33.5	29.3	25.1	20.5	14.5	9.5	5.5
= 30	27.4	27.0	26.4	24.8	22.0	19.3	15.8	11.8	7.3	4.5
= 20	18.4	17.7	17.3	16.5	15.0	12.9	10.5	7.9	4.9	3.0

Table 6. 15. Envelopes of 99 Percentile Wind Speed Change (m/sec), 1- to 80-km Altitude Region, Edwards AFB (From Kaufman¹⁴)

Scales of Distance (m) Thickness										
Wind Speed at Reference Altitude (m/sec)	5000	4000	3000	2000	1000	800	600	400	200	100
≥ 90	77.5	74.4	68.0	59.3	42.8	36.7	30.2	22.5	13.9	8.5
= 80	71.0	68.0	63.8	56.0	40.8	35.0	28.6	21.5	13.2	8.1
= 70	63.5	61.0	57.9	52.0	38.8	33.2	27.0	20.4	12.5	7.7
= 60	57.1	54.7	52.3	47.4	36.0	31.0	25.3	19.0	11.7	7.2
= 50	49.6	47.8	46.2	43.8	33.0	28.3	23.2	17.5	10.7	6.6
= 40	39.4	38.8	37.9	35.5	29.5	25.3	20.6	15.5	9.6	5.9
= 30	30.0	30.0	29.4	26.9	22.6	19.4	15.8	12.2	7.3	4.6
= 20	20.0	19.8	19.5	18.4	15.0	13.1	10.9	9.0	6.3	4.3

Table 6. 16. Envelopes of 99 Percentile Wind Speed Change (m/sec), 1- to 80-km Altitude Region, for All Five Locations (From Kaufman¹⁴)

Scales of Distance (m) Thickness										
Wind Speed at Reference Altitude (m/sec)	5000	4000	3000	2000	1000	800	600	400	200	100
≥ 90	75.2	72.0	67.3	59.0	42.8	36.7	30.2	22.5	13.9	8.5
= 80	68.0	66.3	62.5	55.5	40.8	35.0	28.6	21.5	13.2	8.1
= 70	60.4	59.0	56.8	51.4	38.7	33.2	27.0	20.4	12.5	7.7
= 60	53.0	51.8	49.3	45.0	36.0	30.9	25.2	19.0	11.7	7.2
= 50	44.8	43.6	41.5	38.4	32.0	27.5	22.4	16.9	10.4	6.4
= 40	36.5	35.5	34.5	33.0	27.0	23.2	18.9	14.2	8.8	5.4
= 30	28.0	27.3	26.9	26.3	21.4	18.4	15.0	11.3	6.9	4.3
= 20	18.0	17.7	17.4	16.7	15.2	13.0	10.6	8.0	4.9	3.0

6.4.2 Interlevel Correlations

Deviations in the assumed vertical wind profile over a target or reentry point affect the range and cross-range of a ballistic missile. These effects must be considered in the design of guidance systems for reentry vehicles and for targeting ballistic missiles.

The mean effect, E , of mean monthly or mean seasonal winds on the range and cross-range of a missile can be determined for a particular location by computer-simulated flights through mean monthly component wind profiles if the appropriate influence coefficients for the missile at various levels are given:

$$E = \sum C_i V_i \quad (6.10)$$

where C_i is the influence coefficient at the i th level that describes the portion of the total response of a missile assignable to that level, and V_i represents the mean of the component wind speed at that level. The variation around this average effect caused by day-to-day fluctuations in the winds is obtained from

$$\sigma_{INT}^2 = \sum_{i,j} C_i C_j r_{ij} \sigma_i \sigma_j \quad (6.11)$$

where σ_{INT}^2 is the integrated variance for all levels considered, C_i and C_j are the influence coefficients at the i th and j th levels, σ_i and σ_j are the standard deviations of the component wind at these levels, and r_{ij} is the correlation between the component wind at the i th level and that at the j th level. The square root of the solution to this equation yields the standard deviation for each component of the ballistic wind. The two components can be combined and used to determine the probability of occurrence of deviations of any desired magnitude from a trajectory or impact point based on mean monthly winds. In these computations it is assumed that the cross-component correlations are zero at and between levels and the wind frequency distributions are essentially circular normal.

The wind climatology necessary for determination of ballistic effects consists of statistical arrays of mean monthly north-south and east-west wind components, their standard deviations, and interlevel correlations between the same component at different levels. This information has been prepared in matrix form for a relatively large number of locations. Examples for levels between the surface and 60 km are shown in Table 6.17 for the month of January at Churchill, Wallops Island and Ascension Island. Winds are lighter in summer at middle and high latitudes. For targeting purposes, the wind data must pertain to the locations of interest. For design purposes, however, a representative sample of data from the various climatic regions should be used.

Table 6. 17b. Zonal Winds From the Surface to 60 km at Wallops Island

CORRELATION AT PAIRS OF LEVELS FOR JAN 1969-1976																																				
WALLOPS ISLAND, VA																																				
EAST-WEST WIND M/SEC WEST *																																				
KM KILOMETERS ABOVE SEA LEVEL																																				
MEAN AVERAGE OF OBSERVED VALUES																																				
STDV STANDARD DEVIATION OF VALUES TIMES 10																																				
N NUMBER OF VALUES AT EACH ALTITUDE																																				
KM	0.15	2	4	6	8	10	12	14	16	18	20	22	24	26	28	30	32	34	36	38	40	42	44	46	48	50	52	54	56	58	60					
MEAN	1	12	21	28	34	31	33	28	23	15	11	11	11	14	16	19	24	28	31	34	37	40	45	50	54	57	59	62	63	68	76					
STDV	34	61	90	123	150	120	139	96	88	76	74	81	95	140	174	199	236	254	269	285	279	291	287	308	303	308	290	291	292	282	313					
N	44	44	44	43	41	29	25	22	21	26	21	19	22	42	43	44	44	44	44	44	44	44	44	44	44	44	44	44	44	44	44	44				
2	25	85	34	94																																
4	33	66	55	85																																
6	34	68	55	85																																
8	34	68	55	85																																
10	-4	31	60	77	91																															
12	-21	16	32	44	68	77	87																													
14	-21	17	49	62	83	89	76	66																												
16	-21	17	49	62	83	89	76	66																												
18	-21	17	49	62	83	89	76	66																												
20	-10	-34	-5	12	12	49	52	76	35	93																										
22	-13	-17	5	17	14	57	57	81	89	93	98																									
24	-17	-17	14	18	20	39	45	46	42	47	30	88																								
26	-17	-17	14	18	20	39	45	46	42	47	30	88																								
28	14	16	16	26	32	44	39	27	20	51	17	30	72	89	95																					
30	14	16	16	26	32	44	39	27	20	51	17	30	72	89	95																					
32	14	16	16	26	32	44	39	27	20	51	17	30	72	89	95																					
34	11	16	24	30	37	40	51	42	29	23	23	53	53	73	83	83	95																			
36	8	16	26	37	40	51	42	29	23	23	53	53	73	83	83	95																				
38	3	11	22	30	31	38	46	32	25	29	48	55	66	72	79	86	95																			
40	1	16	29	33	38	28	36	25	12	36	-2	4	33	46	57	60	68	75	84	93																
42	2	13	23	24	20	9	16	6	3	23	-19	-17	18	32	32	41	50	58	68	91	95	96														
44	-2	10	18	17	13	-11	14	9	-5	17	-10	-10	18	22	23	33	41	53	69	86	95	96														
46	-2	10	18	17	13	-11	14	9	-5	17	-10	-10	18	22	23	33	41	53	69	86	95	96														
48	-2	10	18	17	13	-11	14	9	-5	17	-10	-10	18	22	23	33	41	53	69	86	95	96														
50	0	0	6	6	1	-20	-7	7	9	14	-2	-11	-1	-8	-14	-11	-4	4	13	30	50	67	80	89	96											
52	-3	15	12	5	-13	-3	12	13	13	13	-10	-12	-3	-10	-10	-13	-3	4	14	31	51	67	79	87	94	98										
54	-1	13	19	14	-16	-3	12	13	13	13	-10	-12	-3	-10	-10	-13	-3	4	14	31	51	67	79	87	94	98										
56	-1	13	19	14	-16	-3	12	13	13	13	-10	-12	-3	-10	-10	-13	-3	4	14	31	51	67	79	87	94	98										
58	-1	13	19	14	-16	-3	12	13	13	13	-10	-12	-3	-10	-10	-13	-3	4	14	31	51	67	79	87	94	98										
60	8	20	31	26	32	-4	-1	9	2	-8	-6	-13	9	9	12	8	10	16	12	10	39	45	52	68	73	78	84	87	98	98	98	98	98			

** MULTIPLY TABULAR VALUES BY 0.01 TO OBTAIN CORRELATION COEFFICIENTS

6.5 DESIGN DATA ON WINDS

Wind statistics are presented in a variety of ways, each of which is intended for maximum usefulness for particular aspects of design and operational problems. In "Upper Wind Statistics," Crutcher¹⁵ presents northern hemisphere charts of some 15 wind variables or statistics. For surface winds, in the "Climatic Atlas of the United States," the National Weather Service (1968) presents monthly and annual charts of the prevailing direction, mean wind speed, the fastest wind of record and its direction, wind roses that give the frequency distribution of the wind by direction including frequency of calm, the mean wind vector and direction. There is also a table of the frequencies of nine categories of wind speeds (Beaufort) for some 120 U.S. stations.

Generally speaking, any data source on surface wind speed is limited to providing several key parameters, from which the general frequency distribution of the wind, in speed and direction, can be estimated or reconstructed. But to do so, a practical model of the distribution of the wind speed must be adopted. Three such models are: the gamma distribution, Weibull distribution, and the circular normal bivariate distribution. Each has its merits and drawbacks.

6.5.1 Hourly Surface Wind Speeds

The distributions of surface wind speeds, observed every hour on the hour, have been studied by many climatologists and statisticians whose conclusions and consequent models differ. Some favor the distribution of wind speeds as given by the circular bivariate normal distribution, others the log-normal, still others the gamma distribution. A historical record of at least five years should be used to obtain good estimates of wind speed distributions, especially small probabilities (for example, 1 percent). Although there are about 600 city and airport stations in the United States where hourly records are kept, they generally represent wind fields inadequately. A location that is close to a weather reporting station should have similar wind characteristics, but terrain effects, including man-made effects, and proximity to large bodies of water superimpose a spatial variability that is difficult to generalize. Fairbanks, Alaska, for example, has a mean wind speed, in January, of 0.9 mps with standard deviation 1.7 mps. Yet Big Delta, only 121 km away, has a mean wind speed of 5.4 mps and standard deviation 4.9 mps.

The following are alternative models of windspeed frequency distribution:

15. Crutcher, H. L. (1959) Upper Wind Statistics Charts of the Northern Hemisphere, NAVAER 50-IC-535.

Model Alternative 1: A gamma distribution. In terms of the mean wind speed (\bar{V}_s) and standard deviation (s_s), the probability density function of the wind speed (V_s) is given in terms of a transformed variable (y) by

$$f(y) = 0.5 y^2 e^{-y} \quad (6.12)$$

where

$$(y - 3) / \sqrt{3} = (V_s - \bar{V}_s) / s_s \quad (6.13)$$

The cumulative probability of wind speed, $P(V_s)$ equal to or less than V_s is given by

$$P(V_s) = 1 - e^{-y} (1 + y + y^2/2) \quad (6.14)$$

As an example, in the month of January, the noontime Bedford, Mass., wind has a mean hourly speed (\bar{V}_s) of 9.9 knots and standard deviation (s_s) of 6.71 knots. Equation (6.14) gives the cumulative probability for several values of the wind speed as follows:

V_s	y	Estimated $P(V_s)$	Observed Distribution
calm	0.445	0.011	0.115
3 knots	1.219	0.125	0.168
6	1.993	0.321	0.322
10	3.03	0.583	0.592
16	4.57	0.834	0.838
21	5.89	0.932	0.946
27	7.41	0.978	0.989
33	8.96	0.9936	0.999

This kind of approximation is good for moderate to strong wind speeds, and is generally useful except for very light winds or calm conditions.

Model Alternative 2: A Weibull Distribution. A recent study¹⁶ has produced the model

$$P(V_s) = c + (1 - c) \left\{ 1 - e^{-\alpha V_s^\beta} \right\} \quad (6.15)$$

16. Bean, S.J., and Somerville, P.N. (1979) Some Models for Windspeed, Sci. Rpt. No. 4, Contract F19628-77-C-0080, AFGL-TR-79-0180, AD A077048.

where c is the probability of calm, and α , β are parameters of the Weibull distribution that are determined either to make the model fit the observed frequencies of wind speed (in a least squares sense), or are estimated in other effective ways. The records of many stations indicate a high probability of "calm" which makes this formulation desirable.

Records like the "Revised Uniform Summaries of Surface Weather Observations" (RUSSWO)* contain the relative frequencies (f_i) of each of 11 or fewer wind speeds (V_s). Where x_i , the middle value in the category, is used for the i th category of V_s , formulas have been found for α and β as follows:

$$\hat{\alpha} = \Sigma f_i / \Sigma f_i x_i^\beta \quad (6.16)$$

$$\hat{\beta} = [\Sigma f_i \cdot x_i^\beta \ln x_i / \Sigma f_i x_i^\beta - \Sigma f_i \ln x_i / \Sigma f_i]^{-1}$$

To solve for α , β an initial guess is entered for β in the right-hand side of Eq. (6.16), and the equation is solved for a first estimate of β . With this revised estimate the equation is solved again for a second and better estimate, and so on, until the value of β is established.

The RUSSWO for Bedford, Mass., January at noontime, gives f_i for categories of V_s (or x_i) which, when entered in Eq. (6.16) produced the following values after several iterations:

$$\hat{\beta} = 1.961$$

$$\hat{\alpha} = 0.00685 .$$

When these values for α and β are entered in Eq. (6.15) together with $c = 0.115$, the probabilities $P(V_s)$ become:

* Compiled by the Environmental Technical Applications Center, Scott AFB, Ill.

V_s	$P(V_s)$	Observed Distribution
calm	0.115	0.115
3 knots	0.166	0.168
6	0.297	0.322
10	0.527	0.592
16	0.816	0.838
21	0.9395	0.946
27	0.989	0.989
33	0.9987	0.999

Model Alternative 3: The circular normal distribution.

The assumption of the circular normal distribution for the wind implies that the zonal (u) and meridional (v) components each have a normal Gaussian distribution with individual means (\bar{u} , \bar{v}) but with the same standard deviation (s). The two components are independently distributed. As a consequence the probability density function of each is:

$$f(u) = [\exp \{ -(u - \bar{u})^2 / 2 \}] / \sqrt{2\pi} \quad (6.17)$$

$$f(v) = [\exp \{ -(v - \bar{v})^2 / 2 \}] / \sqrt{2\pi}.$$

The magnitude of the mean wind vector (\bar{V}) is given by

$$|\bar{V}| = \sqrt{\bar{v}^2 + \bar{u}^2}. \quad (6.18)$$

The standard vector deviation (s_v) is simply

$$s_v = s\sqrt{2} \quad (6.19)$$

The mean wind speed (\bar{V}_s) and the standard deviation of the wind speed (s_s) are not easily derived from the components. The cumulative probability, $P(V_s)$, of the wind speed, however, can be given in terms of \bar{V} and s or s_v . One of the most applicable formulas is:

$$P(V_s) = e^{-y} \sum_{n=0}^{10} \frac{y^n}{n!} [1 - e^{-x} \sum_{m=0}^n \frac{x^m}{m!}] \quad (6.20)$$

where

$$x = V_s^2 / s_v^2$$

$$y = |\bar{V}|^2 / s_v^2.$$

In the example of Bedford, Mass., January noontime winds, the RUSSWO table of wind speed versus wind direction yields

$$|\bar{V}| = 5.494 \text{ knots}$$

$$s_v = 10.157 \text{ knots}$$

or

$$S = 7.182 \text{ knots (the average of 7.287 and 7.076)}$$

as opposed to

$$V_s = 9.9 \text{ knots}$$

$$s_s = 6.71 \text{ knots.}$$

When the values for $|\bar{V}|$ and s_v are used in Eq. (6.20) the probabilities $P(V_s)$ become:

V_s	$P(V_s)$	Observed
3 knots	0.063	0.168
6	0.231	0.322
10	0.521	0.592
16	0.853	0.838
21	0.964	0.946
27	0.9936	0.989
33	0.9965	0.999

The distribution of the wind (V) around the mean wind vector (\bar{V}) is sometimes of prime interest as it would be in targeting. It is the difference between the actual vector wind and the mean vector wind and has the distribution

$$P(V) = 1 - e^{-V^2 / s^2} \quad (6.21)$$

Thus a circle of radius equal to one standard vector deviation, drawn about the tip of the mean wind vector, would encompass 63 percent of the population of winds. Half of the wind vectors will fall within a circle of radius 0.83 times the standard vector deviation.

6.5.2 Surface Wind Direction

Winds tend to have a modal direction, like the trade winds or the prevailing westerlies. Using the model of the bivariate normal distribution, the estimate of the frequency $P(\theta_1 \leq \lambda < \theta_2)$ of the wind direction (λ) between directions θ_1 and θ_2 is given by

$$P(\theta_1 \leq \lambda < \theta_2) = (1 / \sqrt{2\pi}) \cdot \sum_{u=0}^{u_{\max}} [e^{-\frac{(u-\bar{u})^2}{2}} \delta u] [F(x_2) - F(x_1)] \quad (6.22)$$

where

$$u = V/s,$$

V is the wind component in the direction (θ_0) of the mean wind vector (\sqrt{V}), and s is the standard deviation of the appropriate wind component,

$$u = |\sqrt{V}| / s,$$

δu is a small increment of u ,

$$x_2 = \tan(\theta_2 - \theta_0),$$

$$x_1 = \tan(\theta_1 - \theta_0),$$

and $F(x)$ is approximated by

$$F(x) = 1 - 0.5(1 + c_1x + c_2x^2 + c_3x^3 + c_4x^4)^{-4}$$

where

$$c_1 = 0.196854$$

$$c_2 = 0.115194$$

$$c_3 = 0.000344$$

$$c_4 = 0.019527$$

In the example for Bedford, Mass., January noontime wind $\theta_0 = 300^\circ$. After correcting for calm frequency of 0.115, the computed frequencies of wind directions were as follows:

Direction	$P(\theta_1 \leq \lambda < \theta_2)$	Observed
N	0.082	0.067
NNE	0.056	0.041
NE	0.027	0.040
ENE	0.027	0.013
E	0.022	0.019
ESE	0.019	0.010
SE	0.018	0.014
SSE	0.020	0.009
S	0.025	0.022
SSW	0.032	0.051
SW	0.036	0.067
WSW	0.070	0.063
W	0.098	0.108
WNW	0.122	0.143
NW	0.126	0.110
NNW	0.110	0.106

6.5.3 Surface Wind Gusts

Studies on the relationship of gusts to the steady wind speed are in general agreement; however, quantitative results have varied depending on the data and the analytical methods used. Sissenwine et al,¹⁷ reviewed the results of many of these; he also presented a comprehensive analysis of gustiness based on actual wind records during periods of strong winds, which were observed at 14 airfields in the Northern Hemisphere between 14° and 77° latitude. Tattelman¹⁸ analyzed the same data to develop 50-, 75-, 90-, and 98-percentile gust factor curves for 5-min, 1-min, and 30-sec average (or steady) wind speeds. Gust speeds reported in weather observations are normally considered to be about 2-sec averages, but for designers of various sized equipment, other short duration gusts may be applicable.

Since resolution of the wind records was approximately 2 sec, the shortest period gusts were considered to be 2-sec wind speeds. Gust factor (GF) curves were fitted using the equation

17. Sissenwine, N., Tattelman, P., Grantham, D.D., and Gringorten, I.I. (1973) Extreme Wind Speeds, Gustiness, and Variations With Height for MIL-STD-210B, Air Force Surveys in Geophysics No. 273, AFCRL-TR-73-0560, AD 774044.
18. Tattelman, P. (1975) Surface gustiness and wind speed range as a function of time interval and mean wind speed, J. of Appl. Meteorol. 14(No. 7):1271-1276.

$$GF = 1 + Ae^{-BV}, \quad (6.23)$$

where A and B are constants, and V is the speed of the steady wind. The values for B were determined by a least squares fit of all the data to the 5-min, 1-min, and 30-sec speeds. Using these values of B, the value for A was determined for each percentile curve by a least squares fit to the mid-class wind speed values (for example, 24.5 knots for V = 20-29 knots) and weighted for the number of observations at each point. Figure 6.13 shows curves of the 30-sec gust factor as related to the 5-min steady speed, and the 1-min gust factor related to the 5-min speed using all the data. Figure 6.14 shows the relationship between the 2-sec gust factor and the 5-min steady speed. Curves in both figures extend beyond the limit of the wind data, for which the highest steady speed is 69 knots.

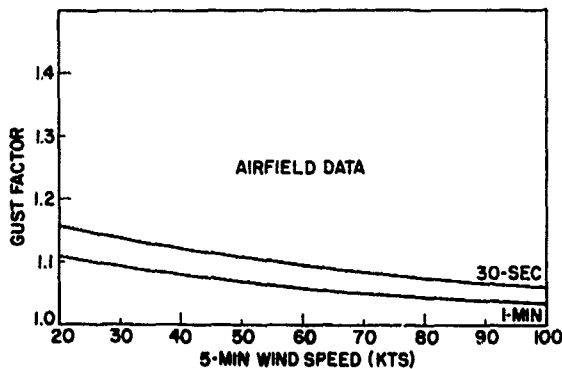


Figure 6.13. Curves of the 30-sec and 1-min Gust Factor to 5-min Wind Speed for the Airfield Data Fitted to $GF = 1 + Ae^{-BV}$

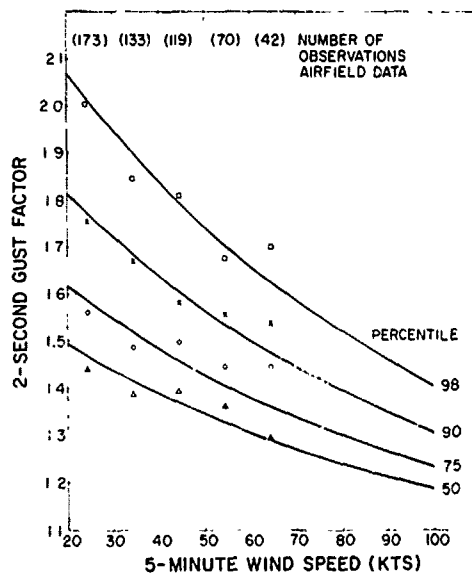


Figure 6.14. Relationship Between the 2-sec Gust Factor and the 5-min Wind Speed at Indicated Percentiles for the Airfield Data (data were fitted to $GF = 1 + Ae^{-BV}$ and weighted for the number of observations at each mid-class value)

Sherlock¹⁹ found that a gust must have a duration such that its size is about eight times the downwind dimension of a structure in order to build a force on the structure commensurate with the gust speed. Because the orientation of most equipment will not be taken into consideration, the shortest horizontal dimension of the equipment should be considered as the downwind dimension. For example, if a structure has a 5-m downwind dimension, a gust must be 40 m long to build up full dynamic pressure. Therefore, a speed of 40 m sec^{-1} (78 knots) would build up full force on such a structure in only 1 sec; a speed of 20 m sec^{-1} would require 2 sec. Figure 6.15 shows the expected (50-percentile) gust factors versus gust duration and 5-min steady speed to aid in calculating the design windspeed for structures of differing downwind dimensions. The curves were drawn to four points: a gust factor of 1.0 at 300 sec, the 60-sec and 30-sec gust factors for each speed from Figure 6.13, and the 2-sec 50-percentile gust factors from Figure 6.14. Lines on Figure 6.15 were extended from the 2-sec gust factors to include 1-sec gust factors.

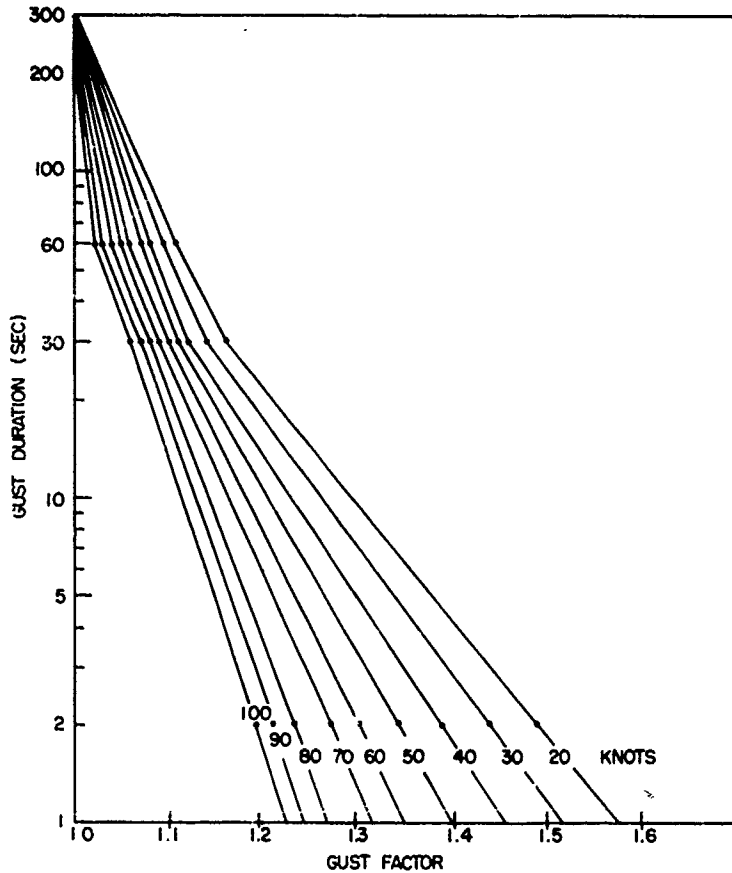


Figure 6.15. Expected (50-percentile) Gust Factors Versus Gust Duration and 5-min Steady Speed

19. Sherlock, R. H. (1947) Gust factors for the design of buildings, Int. Assoc. for Bridge and Structural Engineering, 8:207-235.

Tattelman¹⁸ also presented curves of the 50-, 75-, 90-, and 98-percentile wind speed range (the difference between the maximum and minimum 2-sec speed) as a function of time interval and mean 5-min wind speed. The 90-percentile wind speed range is shown in Figure 6.16. The dashed lines indicate extrapolation beyond the limits of the data. The gust factor and wind speed range curves in this section are considered applicable to most airport locations at the average height of the data used, 15 m (50 ft).

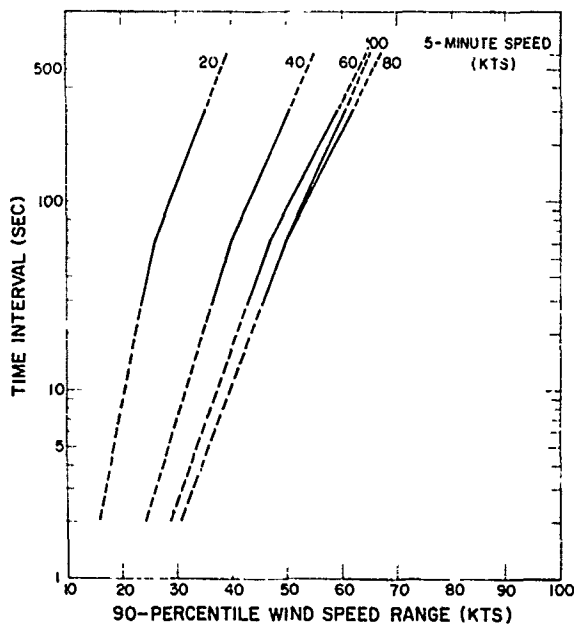


Figure 6.16. Ninety Percentile Wind Speed Range Versus Time Interval and 5-min Speed

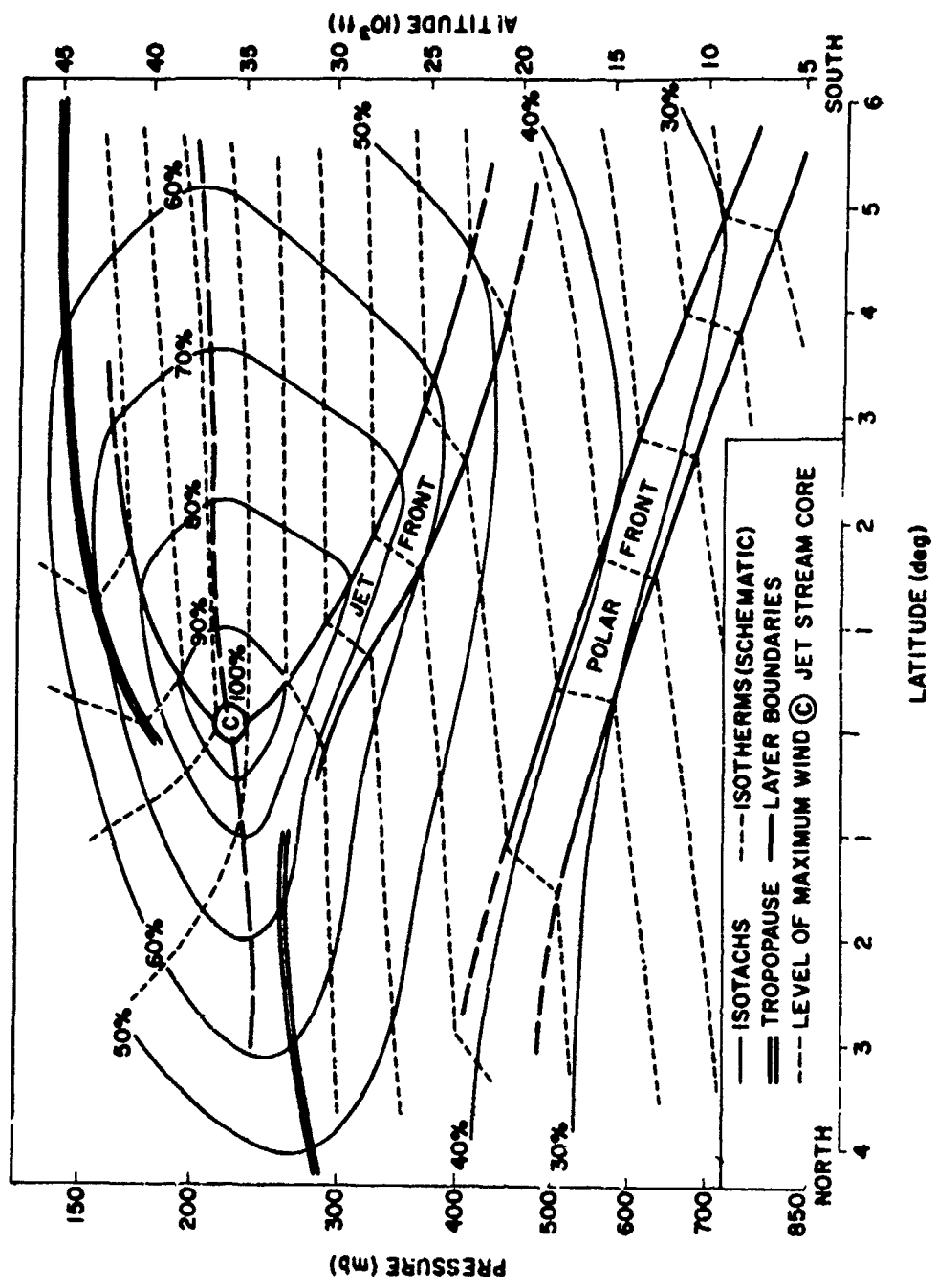


Figure 6. 17. Idealized structure of the Jet Stream, Average Structure in a Cross Section Perpendicular to the Flow (Percent of the core speed is given for each isobar; wind direction is into the page)

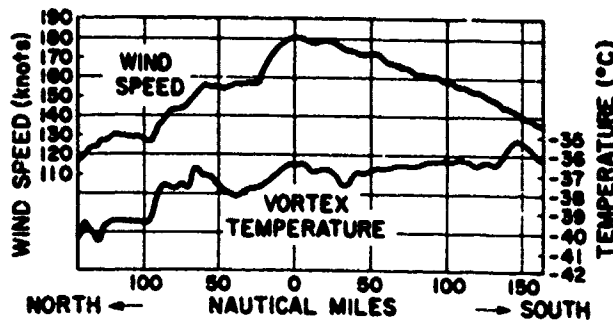


Figure 6.18. Example of Wind and Temperature Fields Near the Jet Stream

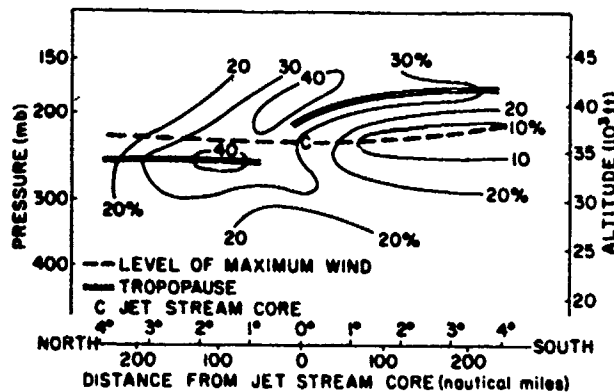


Figure 6.19. Turbulence in Various Sectors of a Typical Jet Stream Cross Section (Frequency (%) of occurrence is shown for each contour)

6.5.4 Extreme Surface Wind Speeds

Various statistics are used for the daily maximum wind speed. One statistic is the maximum 5-min wind of the 288 5-min intervals of one day. Another popular measure is the fastest mile, which is the reciprocal of the shortest interval (in 24 hr) that it takes one mile of air to pass a given point. The strongest gust is the highest reading of an instantaneous recording anemometer. There is no unique relation between these units. The Washington, D. C. records show that, for speeds greater than 15 m sec^{-1} , the maximum 5-min wind speed is roughly 0.93 times the fastest mile and roughly 0.67 times the strongest gust. The maximum 1-min wind speed is roughly 0.71 times the strongest gust. Canadian and British records show the maximum 1-hr wind speed to be 0.62 times the strongest gust.

A model distribution of the annual extreme has been the subject of conflicting viewpoints. The most favored distribution is the Fisher-Tippett Type I, now generally known as the Gumbel Distribution. If x is the symbol for the annual extreme, then the cumulative probability of x is given by

$$P(x) = \exp[-\exp(-y)] \quad (6.24)$$

where y is the reduced variate, whose mean is $\tilde{y} = 0.5772$ and whose standard deviation is $\sigma = 1.28255$.

A relatively simple equation can be used to relate x to y :

$$(y - \tilde{y}) / \sigma_y = (x - \bar{x}) / s_x \quad (6.25)$$

where \bar{x} and s_x are the mean and standard deviation, respectively, of the annual extremes (x).

The work that is implied, to make adequate estimates of percentiles of x , is to find the sample mean and standard deviation of a set of N extremes of N years. Other approaches, although more rigorous, require ordering the N extremes by magnitude and/or estimating parameter values by successive approximations. Estimates also might depend directly on sample size.

If the probability is sought, to judge the risk of an extreme event in n years, then Eq. (6.24) above is replaced by:

$$P(x; n) = \exp[-n \exp(-y)] \quad (6.26)$$

To estimate x for probability P in n years, or an n -year risk $(1 - P)$, knowing the annual extreme mean (\bar{x}) and standard deviation (s_x) from Eq. (6.25);

$$\hat{x} = \bar{x} + s_x (y - \tilde{y}) / \sigma_y \quad (6.27)$$

where

$$y = \ln(n) - \ln(-\ln(P)) \quad (6.28)$$

As an example, a 19-yr record at Denver, Colorado shows an average annual 5-min wind speed maximum, 15 m above ground level, of 19.6 mps and standard deviation 2.53 mps. If a tower is to be built to last for 25 years with 99 percent certainty of survival throughout the 25 years, then the critical wind speed, given by Gumbel model [Eqs. (6.28), (6.27)] is estimated at 33.9 mps.

An estimate is subject to sampling variations, in the above example a 19-yr sample. One standard error of this estimate $s(\hat{x})$ is approximately

$$s(\hat{x}) = s_x \sqrt{\alpha/N}$$

where N is the number of years, and α is given by

$$\alpha = 0.710 + 0.116y + 0.669 y^2 .$$

In the Denver example, the standard error of the estimate (33.9 mps) is approximately $s(\hat{x}) = 3.8$ mps, or 11 percent of the estimate itself. A brief meteorological record of annual extremes permits estimates only within confidence bands that vary with the size of the record.

Publications by climatic agencies such as NOAA Environmental Data Service and the Canadian Meteorological Service give extreme values. Yet each permanent installation might require a special study for a particular site and/or for a particular design problem. For example, the extreme annual wind speed at Logan Airport (Boston) would be an underestimate by about 33 percent, of the extreme on Blue Hill, 19 km to the south-southwest. Even the record at the exact location of interest may not be representative of the wind effects on a tall (or short) structure.

Table 6.18 gives means and standard deviations of annual extreme wind speeds and peak gusts at some representative stations around the world, including stations that are typically in the paths of hurricanes. The 1 percent risk in 10-yr was computed by the above formula, assuming the Gumbel distribution. This column is virtually the same as for the 1000-yr return period, and thus is the speed that has only 1/10 of 1 percent chance of being exceeded each year. There is a noticeable difference between the extreme speeds at airports and at city stations, attesting to the effects of tall buildings in the cities. The reduction of speed might be as high as 55 percent, but averages roughly 25 percent.

Tornadoes are severe whirlwinds, typically a hundred meters in diameter, which fortunately are rare accompaniments of severe thunderstorms. They are most common in Australia and the United States where they number some 140 to 150 per year, most frequent in spring in the plains area of the United States between the Rockies and the Appalachians. The wind speeds are generally less than 110 m/sec^{-1} (250 mph) in the lowest 10-20 m above the ground. Speeds up to 140 m sec^{-1} (300 mph) occur occasionally in very severe tornadoes; higher wind speed estimates are generally suspect (Golden²⁰). These high wind speeds place

20. Golden, J. H. (1976) An assessment of windspeeds in tornadoes, Proc. Symp. on Tornadoes, Texas Tech. Univ., Lubbock, Texas, pp 4-52.

Table 6. 18. Extreme Annual Wind Speed (fastest m/sec) at 15.2 m (50 ft) Above Ground at the Given Stations; A Denotes Airport Station

Station		Years of Record	Mean (m/sec)	S. D. (m/sec)	in 10 yr (m/sec)
Tampa, Fla.	(A)	1941-56	23	3.9	42
Miami, Fla.		1943-58	24	8.0	64
Wilmington, N. C.	(A)	1951-58	30	7.1	65
Hatteras, N. C.		1912-57	28	6.0	58
Dallas, Tex.	(A)	1941-58	23	2.9	38
Washington, D. C.	(A)	1949-58	22	3.8	41
Dayton, Ohio	(A)	1944-58	27	3.8	46
Atlanta, Ga.	(A)	1933-58	22	3.3	39
Abilene, Tex.	(A)	1945-58	28	6.1	59
Columbia, Mo.	(A)	1949-58	25	2.8	39
Kansas City, Mo.		1934-58	25	3.1	40
Buffalo, N. Y.	(A)	1944-58	26	3.7	44
Albany, N. Y.	(A)	1938-58	23	3.8	42
Boston, Mass.	(A)	1936-50	26	5.4	53
Chicago, Ill.	(A)	1943-58	23	2.5	35
Cleveland, Ohio	(A)	1941-58	26	2.6	39
Detroit, Mich.	(A)	1934-58	22	2.6	34
Minneapolis, Minn.	(A)	1938-58	23	5.0	48
Omaha, Nebraska	(A)	1936-58	26	5.9	55
El Paso, Tex.	(A)	1943-58	26	2.0	36
Albuquerque, N. M.	(A)	1933-58	27	4.6	50
Tucson, Ariz.		1948-58	22	3.2	38
San Diego, Calif.		1940-58	16	2.7	30
Cheyenne, Wyo.		1935-58	28	3.1	43
Rapid City, S. D.		1942-58	30	3.0	44
Bismarck, N. D.		1940-58	30	2.3	41
Great Falls, Mont.		1944-54	29	1.6	37
Portland, Ore.		1950-58	25	3.0	41
New York, N. Y.		1949-58	26	2.1	37
Pittsburgh, Pa.		1935-52	23	2.8	37

them outside the distributions discussed previously. Their small dimensions and infrequent occurrence make it impossible to state precise probabilities of occurrence at specific locations. Statistics of occurrence on an areal basis have been developed by Abbey²¹ and Kelly et al.²²

Hurricanes, while much more frequent, and larger and more predictable, still cause problems for the statistical analyst. Recent studies at the National Bureau

21. Abbey, R. F., Jr. (1976) Risk probabilities associated with tornado windspeeds, Proc. Symp. on Tornadoes, Texas Tech. Univ., Lubbock, Texas.

22. Kelly, D. L., Schaeffer, J. T., McNulty, R. P., Doswell, C. A. III, and Abbey, R. F., Jr. (1978) An augmented tornado climatology, Mon. Wea. Rev., 106:1172-1183.

Table 6. 18. Extreme Annual Wind Speed (fastest m/sec) at 15.2 m (50 ft) Above Ground at the Given Station; A Denotes Airport Station (Contd)

Station	Number of Years of Data	Mean (m/sec)	S. D. (m/sec)	in 10 yr (m/sec)
Fairbanks, Alaska	9	17	3.7	35
Nome, Alaska	11	27	4.1	47
Elmendorf AFB, Alaska	14	20	3.2	36
Shemya Island, Alaska	10	31	7.8	45
Hickam AFB, Hawaii	17	20	3.8	38
Clark AB, Philippines	13	17	5.5	45
Lajes Field, Azores	13	28	7.6	65
Albrook AFB, Canal Zone	18	12	1.8	21
San Pablo, Spain	11	34	6.8	68
Wheelus, AB, Libya	14	22	5.3	48
Stuttgart, Germany	15	18	2.1	29
Keflavik, Iceland	9	38	4.8	62
Thule, Greenland	14	36	5.5	63
Tainan, Formosa	39	24	9.5	71
Taipei, Formosa	39	26	9.8	75
Itazuke AB, Japan	14	19	4.5	42
Misawa AB, Japan	11	21	3.2	37
Tokyo Intl. Airport, Japan	15	23	5.5	46
Kimpo AB, Korea	8	19	3.6	37
Bombay, India	6	22	6.3	54
Calcutta, India	6	25	3.3	42
Gaya, India	6	23	3.0	38
Madras, India	6	20	3.4	37
New Delhi, India	6	23	1.7	31
Poona, India	6	17	2.7	31
Central AB, Iwo Jima	17	35	16.9	119
Kadena AB, Okinawa	14	37	11.3	93

of Standards suggest that the Gumbel (Type I) distribution of extreme winds does not provide as good a description of the extreme wind distributions when they must include hurricane winds. The departures of the winds from the Gumbel estimates tend to be on the weaker side. This means that the estimates of Table 6. 18 should be used with caution. Hurricanes may strike at some stations while missing others, so that the record extreme wind speeds of one station may not represent the potential risk of still stronger winds at another nearby station or even at the same station. We conclude, however, that the fit of all data including hurricane winds is best to the Gumbel distribution.

Directly recorded data for record wind extremes are rare due to damage or destruction of the wind measuring instruments, power outages, and so on, during an event such as a tornado or hurricane. Newspaper reports give estimates whose reliability are unknown and variable. Some might be from a weather station where

visually observed wind-speed dials were still in operation even though the recorder lost power. Others might be calculated from the amount of force required to blow over a building or tree or to drive a metal rod through a wooden post.

The recognized worldwide maximum wind speed measured at a surface station is a 5-min speed of 91 mps (177 knots) and a 1-sec gust of 101 mps (196 knots) measured at Mt. Washington, New Hampshire Observatory on 12 April 1934. Mt. Washington is 1915 m above mean sea level and the anemometer was mounted at 11.6 m.

Operationally speaking, the greatest wind extremes are typically in northern Scotland. In the windiest month the 1-percentile is set at 22 mps (a 1-min wind at 3 m above ground level). Gusts accompanying this extreme are estimated, by the shortest dimension of equipment, at

Dimension (m)	Speed (mps)
< 0.6 m	32 mps
1.5	30
3.0	29
7.6	27
15.2	26
30.5	25

6.5.5 Structure of Jet Streams

Belts of exceptionally strong winds are jet streams. (The term as commonly used applies to the strong westerly winds found at the base of the stratosphere.) Because the meteorological disturbances vary in size and intensity and are moving, the jet streams vary in extent, severity, and location. Geographically-oriented descriptions obscures significant features. As Figure 6.17 shows, this is overcome by relating the features to the position of the core. In winter, the centers (or cores) of jet streams are found at altitudes between 9 and 12 km in latitudes 25° to 70° in each hemisphere. In summer, jet streams are weaker, higher (11 to 14 km), and farther poleward (35° to 75° latitude). Generally speaking, a jet stream is several thousand kilometers in length, several hundred kilometers in width, and several kilometers in depth.

The typical structure of jet streams is shown in Figure 6.17; this is a cross section showing isotachs (lines of equal wind speed blowing "into the page") labelled in percent of the wind speed at the jet core. Core wind speeds range from 50 mps to as much as 130 mps on rare occasions. Speeds of 75 mps are common in winter. Figure 6.17 also shows the thermal field, the tropopause, and the level of maximum

wind. Typical wind and temperature variations across jet streams at a constant altitude or vertically through jet streams may be determined from this figure.

Individual jet streams are variable and may differ considerably from the typical. In some cases, two or three jet cores may be found paralleling each other, separated by distances of several hundred kilometers. In addition to these deviations from the average, eddies of various sizes are present in the wind and temperature fields, as shown in Figure 6.18. Extreme horizontal changes of wind and temperature are of the order of 20 mps and 5° C in a 3-km distance measured perpendicular to the jet stream. Variations parallel to jet streams are an order of magnitude smaller.

Clear air turbulence is closely related to jet stream structure; measurements show that it is more likely in certain regions than in others.²³ At the level of maximum wind (where vertical shear changes sign), turbulence was observed about 14 percent of the time. From Figure 6.19 it can be seen that turbulence is most likely to be found north of the jet stream core near the polar tropopause and above the core along the tropical tropopause. Indication of a maximum is also found in the jet stream front.

Other wind currents which exhibit properties similar to those shown in Figure 6.17 are the low-level jet and the tropical easterly jet stream which is observed in certain areas (for example, southern India) at an altitude of about 14 km in summer.

Frequently it is too expensive to design equipment to operate under extreme conditions. In such cases, calculated risks are assumed or alternate methods of operation are devised for periods when such conditions exist. If high wind speeds, or strong shears normally associated with them, adversely affect the operation of a particular vehicle that is released vertically into the atmosphere, it may be desirable to select several release sites spaced far enough apart to ensure that operational conditions will exist above one of the stations when the critical wind speed or shear is exceeded above the others. In such cases, Figure 6.17 will be useful in selecting alternate sites; it indicates the average rate with which wind speed decreases with distance on both sides of the jet stream core. For example, with a 100-mps wind at the jet stream core, Figure 6.17 indicates that, on the average, a belt of winds exceeding 70 mps can be expected to extend more than 300 km south and nearly 200 km north of the core. Consequently, if the maximum wind likely to occur over a region is 100 mps and the vehicle is only designed to withstand speeds up to 70 mps, alternate release sites should be selected at least 640 km apart. As the jet stream axis occasionally approaches a north-south orientation, selected sites should be more than 500 km apart in longitude as well as in latitude.

23. McLean, G. S. (1962) The Jet Stream and Associated Turbulence, Air Force Surveys in Geophysics, No. 140, AFCRL-62-273(I), AD 275857.

References

1. Naval Oceanography Command, Detachment (1980) Guide to Standard Weather Summaries and Climatic Services, NAVAIR 50-1C-534, Asheville, N. C.
2. Lattau, H. H., and Davidson, B. (Eds.) (1957) Exploring the Atmosphere's First Mile, Pergamon Press.
3. Sherlock, R. H. (1952) Variation of wind velocity and gusts with height, Paper No. 2553, Proc. Am. Soc. Civil Eng. 1:463-508.
4. Shellard, H. C. (1965) The estimation of design wind speeds, Wind Effects on Buildings and Structures, National Physics Laboratory Symposium 16:30-51.
5. Izumi, Y. (1971) Kansas 1968 Field Program, ERP No. 379, AFCRL-72-0041, AD 739165.
6. Kantor, A. J., and Cole, A. E. (1980) Wind Distributions and Interlevel Correlations, Surface to 60 km, ERP No. 713, AFGL-TR-80-0242, AD A092670.
7. Gage, K. S., and Balsley, B. B. (1978) Doppler radar probing of the clear atmosphere, Bull. Amer. Meteor. Soc. 59:1074-1092.
8. Green, J. L., Gage, K. S., and Van Zandt, T. E. (1979) Atmospheric measurements by VHF pulsed Doppler radar, IEEE Trans. Geophys. Electr. GE-17:262-280.
9. Balsley, B. B., and Gage, K. S. (1980) The MST radar technique: Potential for middle atmospheric studies, Pure and Appl. Geophys. 118:452-493.
10. Rottger, J. (1979) VHF radar observations of a frontal passage, J. Appl. Meteor. 18:85-91.
11. Arnold, A., and Bellucci, R. (1957) Variability of Ballistic Meteorological Parameters, Tech. Memo. No. M-1913, Ft. Monmouth, N. J., U.S. Army Sig. Eng. Lab.
12. Ellsaesser, H. W. (1960) Wind Variability, AWS Tech Rept. No. 105-2, Hdqts. Air Weather Service, Scott AFB, Illinois.
13. Fichtl, G. H. (1972) Small-scale wind shear definition for aerospace vehicle design, Jour. of Spacecraft and Rockets 9:79.

References

14. Kaufman, J.W. (Ed.) (1977) Terrestrial Environment (Climatic) Criteria Guidelines for Use in Aerospace Vehicle Design, NASA Technical Memorandum 78118, MSFC.
15. Crutcher, H.L. (1959) Upper Wind Statistics Charts of the Northern Hemisphere, NAVAER 50-1C-535.
16. Bean, S.J., and Somerville, P.N. (1979) Some Models for Windspeed, Sci. Rpt. No. 4, Contract F19628-77-C-0080, AFGL-TR-79-0180, AD A077048.
17. Sissenwine, N., Tattelman, P., Grantham, D.D., and Gringorten, I.I. (1973) Extreme Wind Speeds, Gustiness, and Variations With Height for MIL-STD-210B, Air Force Surveys in Geophysics No. 273, AFCRL-TR-73-0560, AD 774044.
18. Tattelman, P. (1975) Surface gustiness and wind speed range as a function of time interval and mean wind speed, J. of Appl. Meteorol. 14(No. 7):1271-1276.
19. Sherlock, R.H. (1947) Gust factors for the design of buildings, Int. Assoc. for Bridge and Structural Engineering, 8:207-235.
20. Golden, J.H. (1976) An assessment of windspeeds in tornadoes, Proc. Symp. on Tornadoes, Texas Tech. Univ., Lubbock, Texas, pp 5-42.
21. Abbey, R.F., Jr. (1976) Risk probabilities associated with tornado windspeeds, Proc. Symp. on Tornadoes, Texas Tech. Univ., Lubbock, Texas.
22. Kelly, D.L., Schaeffer, J.T., McNulty, R.P., Doswell, C.A. III, and Abbey, R.F. Jr. (1978) An augmented tornado climatology, Mon. Wea. Rev., 106:1172-1183.
23. McLean, G.S. (1962) The Jet Stream and Associated Turbulence, Air Force Surveys in Geophysics, No. 140, AFCRL-62-273(I), AD 275857.